MONITORING FOOD FRESHNESS USING A MULTILAYER COLORIMETRIC SENSOR FILM

A THESIS SUBMITTED TO
THE GRADUATE SCHOOL OF NATURAL AND APPLIED SCIENCES
OF
MIDDLE EAST TECHNICAL UNIVERSITY

BY

CANSU OKTAY

IN PARTIAL FULFILLMENT OF THE REQUIREMENTS
FOR
THE DEGREE OF MASTER OF SCIENCE
IN
FOOD ENGINEERING

MARCH 2023

Approval of the thesis:

MONITORING FOOD FRESHNESS USING A MULTILAYER COLORIMETRIC SENSOR FILM

submitted by **CANSU OKTAY** in partial fulfillment of the requirements for the degree of **Master of Science** i**n Food Engineering, Middle East Technical University** by,

Prof. Dr. Halil Kalıpçılar
Dean, Graduate School of **Natural and Applied Sciences** _____

Prof. Dr. Hami Alpas
Head of the Department, **Food Engineering, METU** _____

Assist. Prof. Dr. Leyla Nesrin Kahyaoğlu
Supervisor, **Food Engineering, METU** _____

Assoc. Prof. Dr. Mehran Moradi
Co-Supervisor, **Food Hygiene, Urmia University** _____

Examining Committee Members:

Prof. Dr. Serpil Şahin
Food Engineering, METU _____

Assist.Prof.Dr. Leyla Nesrin Kahyaoğlu
Food Engineering, METU _____

Prof.Dr. Servet Gülüm Şumnu
Food Engineering, METU _____

Assist. Prof. Dr. Elif Yolaçaner
Food Engineering, Hacettepe University _____

Assoc. Prof. Dr. Mehran Moradi
Co-Supervisor, Food Hygiene, Urmia University _____

Date: 28.03.2023

I hereby declare that all information in this document has been obtained and presented in accordance with academic rules and ethical conduct. I also declare that, as required by these rules and conduct, I have fully cited and referenced all material and results that are not original to this work.

Name Last name : Cansu Oktay

Signature :

ABSTRACT

MONITORING FOOD FRESHNESS USING A MULTILAYER COLORIMETRIC SENSOR FILM

Oktay, Cansu

Master of Science, Food Engineering

Supervisor: Assist.Prof.Dr. Leyla Nesrin Kahyaoğlu

Co-Supervisor: Assoc.Prof.Dr. Mehran Moradi

January 2023, 74 pages

Foodborne diseases might result in serious health problems and correspondingly huge economic and social burdens. Thus, cost-effective and safe advanced sensing materials/schemes are still in great demand to ensure food safety, particularly through user-friendly and cost-effective smart packaging technologies. In this sense, biomaterials can be used safely in smart food packaging applications while improving the structural and physical properties of packaging materials. Multilayer intelligent freshness labels based on bacterial nanocellulose (BNC), polyvinyl alcohol (PVA), and anthocyanins doped zeolitic imidazolate framework-8 (GSE@ZIF-8) nanocrystals were fabricated in this study. BNC was used for the inner layer of the multilayer system to create a highly porous fibrous matrix, which facilitated the diffusion of the released gases as a result of spoilage to reach anthocyanin (GSE) encapsulated ZIF-8. The outer protective layer was fabricated from PVA to ensure optical transparency and provide a support layer for

anthocyanins doped ZIF-8. First, optical, structural, thermal, and surface characterizations of GSE@ZIF-8 nanocrystals were carried out and the successful incorporation of anthocyanins into ZIF-8 nanocrystals was illustrated. Next, GSE@ZIF-8 was introduced into PVA, and multilayer films were fabricated by spin-coating of PVA/GSE@ZIF-8 layers onto BNC. The influence of the deposition cycle numbers on the barrier, mechanical, thermal, morphological, and colorimetric properties of multilayer labels was examined. The ammonia sensing range, and mechanical and barrier properties of the films were demonstrated to be controlled by the number of the PVA/GSE@ZIF-8 layers on the BNC. BNC-2PVA/GSE@ZIF-8 films showing the best colorimetric sensitivity towards volatile ammonia were tested with skinless chicken breasts to monitor the freshness. The changes in the ΔE and a* values of BNC-2PVA/GSE@ZIF-8 film were in line with the microbial growth and TVB-N release in food samples during 10 days of storage at 4 ºC. Taken together, the synthesized multilayer BNC-2PVA/GSE@ZIF-8 film can distinguish the fresh and spoiled chicken meat during storage at 4 ℃ without destructive testing.

Keywords: Bacterial nanocellulose, ZIF-8, Anthocyanins, Spin coating, Intelligent food packaging

ÖZ

ÇOK KATMANLI KOLORİMETRİK SENSÖR FİLM KULLANARAK GIDA TAZELİĞİNİ İZLEME

Oktay, Cansu

Yüksek Lisans, Gıda Mühendisliği

Tez Yöneticisi: Assist.Prof.Dr. Leyla Nesrin Kahyaoğlu

Ortak Tez Yöneticisi: Assoc.Prof.Dr. Mehran Moradi

Ocak 2023, 74 sayfa

Gıda kaynaklı hastalıklar ciddi sağlık sorunlarına ve buna bağlı olarak büyük ekonomik ve sosyal yüklere neden olabilir. Bu nedenle, özellikle kullanıcı dostu ve uygun maliyetli akıllı paketleme teknolojileri yoluyla, gıda güvenliğini sağlamak için uygun maliyetli ve güvenli gelişmiş algılama malzemeleri/planları hâlâ büyük talep görmektedir. Bu anlamda biyomalzemeler, ambalaj malzemelerinin yapısal ve fiziksel özelliklerini iyileştirirken akıllı gıda paketleme uygulamalarında güvenle kullanılabilir. Bu çalışmada bakteriyel nanoselüloz (BNC), polivinil alkol (PVA) ve antosiyanin katkılı zeolitik imidazolat-8 (GSE@ZIF-8) nanokristallerine dayalı çok katmanlı akıllı tazelik etiketleri üretildi. BNC, bozulma sonucu açığa çıkan gazların antosiyanin (GSE) kapsüllenmiş ZIF-8'e ulaşması için difüzyonunu kolaylaştıran oldukça gözenekli bir lifli matris oluşturmak için çok katmanlı sistemin iç katmanında kullanıldı. Dış koruyucu tabaka, optik şeffaflığı sağlamak ve ZIF-8

katkılı antosiyaninler için bir destek tabakası sağlamak üzere PVA'dan imal edilmiştir. İlk olarak, GSE@ZIF-8 nanokristallerinin optik, yapısal, termal ve yüzey karakterizasyonları gerçekleştirildi ve antosiyaninlerin ZIF-8 nanokristallerine başarıyla dahil edilmesi gösterildi. Daha sonra, GSE@ZIF-8, PVA'ya dahil edildi ve çok katmanlı filmler, PVA/GSE@ZIF-8 katmanlarının BNC üzerine döndürülerek kaplanmasıyla üretildi. Biriktirme döngü sayılarının çok katmanlı etiketlerin bariyer, mekanik, termal, morfolojik ve kolorimetrik özellikleri üzerindeki etkisi incelenmiştir. Filmlerin amonyak algılama aralığı, mekanik ve bariyer özelliklerinin BNC üzerindeki PVA/GSE@ZIF-8 katmanlarının sayısı ile kontrol edildiği gösterildi. Uçucu amonyağa karşı en iyi kolorimetrik hassasiyeti gösteren BNC-2PVA/GSE@ZIF-8 filmleri, tazeliğini izlemek için derisiz tavuk göğsü ile test edildi. BNC-2PVA/GSE@ZIF-8 filminin ΔE ve a* değerlerindeki değişimler, 4 ºC'de 10 günlük depolama süresince gıda numunelerindeki mikrobiyal büyüme ve TVB-N salınımı ile uyumluydu. Birlikte ele alındığında, sentezlenmiş çok katmanlı BNC-2PVAGSE@ZIF-8 filmi, taze ve bozulmuş tavuk etini 4°C'de depolama sırasında tahribatlı testler olmadan ayırt edebilir.

Anahtar Kelimeler: Bakteriyel nanoselüloz, ZIF-8, Antosiyanin, Döndürmeli kaplama, Akıllı paketleme

To my Family,

ACKNOWLEDGMENTS

I would like to express my deepest gratitude to my supervisor Assist.Prof.Dr. Leyla Nesrin Kahyaoğlu and co-supervisor Assoc. Prof. Dr. Mehran Moradi for their guidance, advice and assistance throughout the research.

I would like to thank my laboratory colleagues and friends, Beyza Kılıç, Ecem Kaya and İdil Kit, for their precious suggestions.

I also would like to thank to my dearest friends İpek Balta, Fatma Özdemir and Anıl Çakar for their endless support and encouragement.

This work is supported by the Scientific and Technological Research Council of Turkey under grant number TUBİTAK 119N717.

Lastly, I especially want to thank my family Vahide Oktay, Abdullah Oktay and Ece Oktay. I am grateful for their love, encouragement and supports.

TABLE OF CONTENTS

LIST OF TABLES

TABLES

LIST OF FIGURES

FIGURES

CHAPTER 1

INTRODUCTION

1.1. Food Safety

Food safety is a primary concern worldwide and one of the most essential purposes of food legislation. The majority of the foods are perishable and prone to spoilage. The challenges of food safety involve biological hazards, chemical reactions, and improper environmental hygiene conditions (Focker et al., 2022). European Food Safety Authority (EFSA), Food and Drug Administration (FDA), and the United States Centers for Disease Control and Prevention (CDC) are the authorities to take precautions, and regulate food safety in Europe (EU) and the United States (US) (Realini & Marcos, 2014). Nowadays, foodborne diseases are caused mainly by microbial risks associated with food products. According to CDC (2020), nearly 76 million people in the US are affected by foodborne illnesses every year. Approximately 325,000 of the affected people are hospitalized, and consequently, foodborne diseases lead to 5,000 deaths each year (Han et al., 2018). Besides, Listeriosis is the most common foodborne disease in Europe with a significant mortality rate of 13%. It causes serious concerns since Listeria monocytogenes can grow at refrigeration conditions (around 4 °C). Ready-to-eat foods with longer shelf-life, meat and fish products are the foods that are considerably affected by the occurrence of *L. monocytogenes* (Realini & Marcos, 2014). Safe food means improved population health and, thereby enhanced economic conditions. From that perspective, food safety practices and improvements enhance the economic growth of the region (Fung, Wang & Menon, 2018). According to the report of the US Economic Research Service, the economic loss caused by the most common 15 foodborne microorganisms was around 17.6 billion dollars in 2018 (Hoffmann & Ahn, 2021). Overall, health issues are not the only burden of food safety, economic challenges have a significant impact on individuals and governments.

1.2. Food Packaging

The main role of food packaging is to protect food from physical, biological, and chemical damage and contamination by enclosing the food material. Maintaining the quality and safety of food products while storing and transferring is the key responsibility of a package (Han et al., 2018). In addition, the food package provides communication with the consumer, helps the marketing of the product, and lowers economic losses. Successful product protection can be ensured by combining four significant elements: containment, convenience, protection, and communication (Ramos et. al., 2018).

Technology for food packaging is constantly changing in response to the increasing demands of modern society. Legislation, convenience, longer shelf lives, healthier and safer foods, environmental issues, and food wastage problems are some of the most present and upcoming difficulties in the packaging of fast-moving products (Realini & Marcos, 2014). Along the whole food supply chain, an increasing amount of food is lost each year. The estimated amount of food waste is around 89 million tonnes in Europe according to European Commission (2012). For raw meat products, the loss due to spoilage during production and supply chain operations is approximately 40% of the total (Realini & Marcos, 2014). In order to decrease food waste, some optimization techniques for packaging could be developed. These techniques include changing package sizes to encourage consumers to buy foods in proper amounts and preparing new designs to preserve food quality and safety (Lalpuria, Anantheswaran & Floros, 2012). These new designs require suitable technologies to be used in food packages. Those innovations could be successfully integrated into the food industry when they appropriately comply with regulatory requirements and provide profitable outcomes. Additionally, by taking into account a wide range of sustainability challenges such as the use of resources, recycling, and process optimizations, food packaging technologies should also attempt to reduce the environmental burden (Shao et al., 2021). Therefore, innovative packages provide not only technological improvements to the basic functions of packaging but also contribute to a sustainable environment.

1.3. Smart Packaging

Systems for smart food packaging offer improved functionality and they consist of two subgroups, namely, active and intelligent packaging. Active packaging provides functional characteristics like microbiological, temperature, moisture, gas, flavor, and chemical controllers. On the other hand, intelligent packaging uses features such as pH, temperature, time, and gas indicators to communicate environmental changes and indicate the food status (Schaefer & Cheung, 2018). According to Vanderroost et al. (2014), smart packaging offers a comprehensive packaging solution. In addition to monitoring changes in a product and its environment, it also takes appropriate action in response to these changes. The conditions being monitored or the functionalities used in a smart system vary depending on the type of product and its storage conditions.

1.4. Intelligent Packaging

Intelligent packaging is a system that monitors the condition of a food product or the environment that surrounds the food. This system can be used to detect, record, trace, and communicate information on food quality and state throughout the food supply chain (Yam, 2012). Since the package and the food are close together in the whole chain cycle, the package provides the best opportunity for communicating about the food's status. If a package is able to inform people, it is referred to "intelligent".For instance, an intelligent package consists of an indicator for monitoring food safety or quality and provides an early alert to consumers or producers/suppliers. Therefore, this packaging system represents a significant advancement in reducing food waste and enhancing the logistics and traceability of food. Sensors or devices that can indicate the information are used to provide intelligent functionality. Indicators can be divided into two subgroups "external indicators" and "internal indicators" (Sundramoorthy et al., 2018). Time and temperature indicators are examples of external indicators which are positioned outer side of the package. On the other hand, internal indicators inside the package consist of carbon dioxide, microbial growth, or

pathogen indicators(Vanderroost et al., 2014). Further, intelligent packaging technologies contribute to quality analysis and hazard analysis systems that are designed to detect unsafe food, specify possible hazards, and produce solutions to decrease them.

1.5. Freshness Indicators

Freshness indicators that can be found on the cover of the food package are direct indicators of food quality. These indicators in general concentrate on detecting changes in gas composition. Typically, freshness indicators show a permanent color change that is easily recognized by consumers (Vanderroost et al., 2014). Most of them have relied on detecting volatile metabolites produced during food storage, including ammonia, amines, diacetyl, or hydrogen sulfide (Shao et al., 2021). The other part of freshness indicators reacts to biogenic amines and organic acids produced by the microbial breakdown of protein-rich foods (Becerril et al., 2021). For nondestructive testing of the freshness of food items which are seafood, meat products, fruits and vegetables, and dairy products, freshness indicators are a suitable option. Despite these benefits, freshness indicator applications as novel intelligent packaging techniques are currently not common in the food industry.

For the food industry to successfully develop and implement a freshness indicator, it should fulfill a number of requirements (Yam, 2012). Firstly, it must perform fast and sensitive monitoring of deteriorations in the selected compounds with a high correlation between the changes and product quality. Secondly, it must be easy to be used in the food sector by using simple techniques and low costs. The last one is a straightforward reading and understanding by consumers without using special equipment. The final requirement is mostly provided by colorimetric indicators, which is the primary factor of the rapid advancement of this type of technology.

One method for tracking food deterioration includes using pH-sensitive dyes as a freshness indicator, which may be applied to a variety of foods such as fish, meat, and dairy products (Becerril et al., 2021). A pH change occurs when a particular food starts to be spoiled; a pH indicator that is placed in solid support or on the packing

material can track this change. The majority of pH-based freshness indicators are colorimetric sensors since changes in the pH typically result in a color change. This method has been applied frequently to raw fish or meat products because, when they rot, the pH rises due to the development of spoilage microorganisms that produce nitrogen compounds (Balbinot-Alfaro et al., 2019).

Although most of the pH-based freshness indicators are employed with synthetic dyes, research has been done recently to replace these dyes with natural pH indicators, particularly anthocyanin-containing plant extracts (Becerril et al., 2021). Anthocyanins are a good alternative to synthetic dyes since they are easy to obtain, widely distributed in nature, and inexpensive in addition to their natural origin. As anthocyanin toxicity has not been demonstrated in previous studies and the most recent evaluation from EFSA about the Scientific Panel of Food Additives and Nutrient Sources, anthocyanins (mostly grape-skin and black currant extracts) were considered unlikely to be of safety concern, they also avoid the toxicity issues associated with the use of synthetic dyes (EFSA, 2013).

1.5.1. Anthocyanins

The most significant vascular plant pigments are anthocyanins which are responsible for blue, orange, violet, red, and pink hues seen in many plant species like berries, flowers, etc. (Castaneda-Ovando, Pacheco-Hernandez, Paez-Hernandez, Rodriguez,& Galan-Vidal, 2009). Chemically, the flavylium cation serves as the structural foundation for the phenolic compounds known as flavonoids, including these water-soluble colors. Anthocyanidin, a primary component of anthocyanins, is made up of two aromatic rings connected by an oxygenated heterocycle and can form bonds with a variety of sugar moieties. The anthocyanin's chromophore moiety, the flavylium ion, is what gives these pigments their extreme instability and vulnerability to deterioration. There are currently 23 distinct anthocyanidins that have been identified, each having a different number and level of hydroxyl groups in one of the rings that have been methylated. The six anthocyanins found in vascular plants most frequently are pelargonidin, cyanidin, delphinidin, malvidin, peonidin, and petunidin

(Clifford, 2000). More than 500 varieties of anthocyanins have been reported. Their primary distinctions include the number of hydroxylated groups, kind, and bound sugars, and the quantity and placement of aliphatic and aromatic carboxylates attached to the sugar molecules. These variances cause further changes in stability and colors. Light is one of the most significant environmental elements that affect the production of anthocyanins, and the relative abundance of anthocyanins changes substantially depending on the plant species, the time of harvest, or growth circumstances (Tsuda, 2012).

Researchers, businesses, and consumers are very interested in using anthocyanins in the food industry and products because of their color spectrum, great water solubility, as well as their natural origins, and non-toxicity. In various types of processed foods and beverages nowadays, anthocyanins have been frequently utilized as food colorants in place of earlier pigment compounds with synthetic origins (Wallace & Giusti, 2019). Additionally, anthocyanins can be employed in food goods as antioxidants either by adding them directly to the product or by including them in the packaging (Wang Yong et al., 2019). The use of anthocyanins as a food additive is supported by their demonstrated health advantages, which include anti-inflammatory, antioxidant, anti-obesity, anticancer, antibacterial, neuroprotective, and immunomodulatory activities(Li, Wu, Fu, & Reddivari, 2019).

Anthocyanins are unstable since the flavylium ion is present and has an unusual electron distribution (Smeriglio et al., 2016). This instability in addition to the unfavorable interactions with food items constrains the usage of anthocyanins in the food sector. Since it has been demonstrated that an increase in methoxyl groups improves stability while an increase in hydroxyl groups has the opposite effect, the chemical structure of anthocyanins is crucial to their stability (Becerril et al., 2021). In addition, glycosyl acylation of anthocyanins has been shown to increase the chemical stability of anthocyanins both *in vitro* and *in vivo* (Zhao et al., 2017). As to generate extracts with a high level of chemically stable anthocyanins, it is crucial to choose the raw material source of the plant properly. Because they contain significant levels of stable acetylated anthocyanins, black carrots, red cabbage, and purple sweet potatoes are now widely used as sources of anthocyanins (Zhao et al., 2017). When anthocyanins interact with other anthocyanins, metallic ions, phenolic compounds,

and other non-phenolic components such as pectin or other hydrocolloids such as polysaccharides, as happens in nature, their stability is increased (Castañeda-Ovando et al., 2009). These linkages not only improve stability but also have the potential to alter or increase color intensity. The final colors that plants display in nature are primarily due to a phenomenon known as copigmentation. The food sector may also employ interactions to enhance the stability and color features of the extracts. To prevent high degradation rates of anthocyanins and to achieve high yields, suitable anthocyanin extraction techniques must be used. The traditional methods rely on an extraction step using a solvent, often one of the polar kind like methanol, ethanol, acetone, or water, which has been acidified using a wide range of organic and inorganic acids. Attempts have been made to employ alternative, more favorable contemporary procedures to minimize the amount of solvent used, enhance the kinetics of the extraction, eliminate the need for purification and concentration stages, or boost the extraction yield (Mohammad, 2021). Among these, pressured liquid extractions, microwave and ultrasound assistance, and microwave assistance have all shown significant promises for the extraction of anthocyanins. Despite this, these methods are ineffective and should be used at low temperatures to prevent the deterioration of anthocyanins (Silva et al., 2017).

Anthocyanins in the solution can be found in several chemical forms depending on the pH because of their ionic structure. Besides, significant effects on the stability and hue of anthocyanins result from this ionic structure. It is generally acknowledged that the dominating species at low pH exhibit substantially better stability than the more prevalent species at higher pH values (Azlan, Tang, & Lim, 2017). Regarding color, many shades that have been seen for the various species cause them to behave as pH indicators that are seen in nature. At low pH, anthocyanins often exhibit red colors, whereas, at increasing pH, the color spectrum shift to purple and blue colors (Cavalcanti, Santos, & Meireles, 2011). This specific characteristic of anthocyanins has been the most important reason for them being utilized as freshness indicators in the fabrication of colorimetric films.

1.5.2. Other Pigments used in Freshness Indicator

Carotenoids are lipophilic pigments that give plants like corn, carrots, papayas, tomatoes, and watermelons their yellow, orange, and red hues, and some fish like salmon and crustaceans such as cooked lobster and shrimp their red hue (Rodriguez-Amaya, 2018). There are more than a thousand different forms of carotenoids; the most common ones include b-carotene, lycopene, lutein, astaxanthin, bixin, norbixin, and zeaxanthin (Burri, 2013). The structure of the carotenoids varies and are typically made up of eight isoprenoid subunits and have a conjugated double bond that serves as a chromophore in the center of their structure. That double bond is important for carrying out the bioactive and colorimetric functions of carotenoids as the activity of the lipophilic pigment is linked to antimicrobial and antioxidant characteristics (Martins, Santos, Romani & Fernandes, 2022). Like other natural coloring pigments, carotenoids are vulnerable to isomerization, oxidation, and degradation by enzyme activities and exposure to pH, oxygen, light, and temperature. The main structural alterations in carotenoids occur during oxidation and geometrical isomerization, which cause the double bond to be broken and the chromophore molecule to be lost, resulting in a shift in color from intense orange to pale yellow (Santos-Zea et al, 2019). Carotenoids are frequently employed in assessing the quality and freshness of frozen fish or poultry products because of their susceptibility to color change due to exposure to poor storage temperature settings (Martins et al., 2022).

Betalains are water-soluble coloring pigments that are obtained by betalamic acid and are commonly observed in plants (Liu et al., 2022). Red pitaya, beetroot, prickly pear, and amaranth are the major sources of betalains which have two main subgroups: betacyanins and betaxanthins. Betacyanins are reddish-violet colored because of the reaction between cyclo-dopa and betalamic acid. Nevertheless, once betacyanins are linked to amines or amino acids, they form yellow-colored betaxanthins (Martins et al., 2022). The molecular structure and color of betalains change when the alkalinity of the environment rises and also with the change in light and temperature (Calva-Estrada, Jimenez-Fernandez & Lugo-Cervantes, 2022). Recent research has established the antibacterial, anticancer, and lipid-lowering effects of betalains

(Gandía-Herrero, Escribano & García-Carmona, 2016). Given their antibacterial, antioxidant, and pH-dependent color-changing qualities, they can be used to create active packaging and intelligent packaging (Rodriguez-Amaya, 2018).

Curcumins are widely used in the food industry and can be extracted from *Curcuma* species. They are hydrophobic diphenolic dyes with excellent anti-inflammatory, antibacterial and antioxidant properties (Liu et al., 2022). The formation of curcumin occurs by two metoxyphenol groups joining with the help of ß-diketone moiety (Martins et al., 2022). The stability of curcumin is pH-dependent.In lower pH values than 7 (acidic conditions), the dominant structure is keto tautomerism, which produces a bright yellow color (Jiang, Gosh & Charcosset, 2021). When curcumin is in alkaline conditions, the enol form is predominated, which is characterized by a red or brown hue (Liu, Smart, Pannala, 2020). As a result, curcumin has demonstrated significant potential in the use and advancement of colorimetric indicators, with the ability to identify signs of probable food degradation, such as pH change and increased volatile amine concentrations (Martins et al., 2022).

The green color of fruits and vegetables is a result of chlorophylls. Chlorophylls are present in cyanobacteria, algae, and plants (Alizadeh-Sani et al., 2020). The four pyrrole rings that make up a chlorophyll molecule are joined by a central atom of magnesium and a hydrophobic phytol group (Villao et al., 2015). The effects of heat, light, age, and oxygen on these pigments (Santos-Zea et al., 2019). Chlorophyll degrades as a result of processes like the aging of green vegetables and heat processes. Chlorophylls' color variations are influenced by pH and temperature; as a result, they can be used to track changes in temperature (MacIel et al., 2012).

1.6. Polymers and Food Packaging

Polymers are large molecular materials that consist of monomer chains or rings. Natural polymers are obtained from natural sources and synthetic polymers are based on petroleum (Annu, Akbar & Ahmed, 2021). Both natural and synthetic polymers are commonly used in food packaging due to their beneficial qualities. Most of these polymers show good barrier, thermal and mechanical characteristics and have easy applicability and lower costs (Abdullah & Dong, 2019). In other words, polymers are widely used since they are flexible, light weighted, and easily shaped with lots of different applications such as extrusion, lamination, and blowing. Being able to have different shapes provide a possibility for uniquely shaped foods to be packaged. Moreover, owing to their barrier qualities, which help to maintain product freshness, prevent contamination, and extend shelf life, polymer materials are suitable for many aspects of food packaging.

Polymers are the most common materials used in food packaging applications. Despite their beneficial qualities, petroleum-based synthetic polymers contribute to environmental problems (Annu, Akbar & Ahmed, 2021). Processing and manufacturing of polymeric materials are energy-intensive processes that produce a significant amount of greenhouse gases and contribute considerably to global warming. In addition, the wastes of petroleum-based synthetic polymers have been an important problem for many years. According to Yadav et al.(2018), burning polymer plastics releases toxic emissions that seriously affect the environment and public health. Therefore, the usage of environmentally friendly packages instead of petroleum-based polymers has increased recently. Unfortunately, natural polymers have some inherent limitations such as high permeability, brittleness, poor processing stability, and low resistance to heat. These drawbacks can be solved by mixing them with other polymers and/or strengthening them with nanofillers (Sorrentino et al., 2007).

1.6.1. Synthetic Polymers

Synthetic polymers generally derive from petroleum in a controlled condition, and their main structural component is a network of carbon-carbon bonds. The chemical bonds that keep monomers together are altered by pressure and heat in the presence of a catalyst, leading the monomers to bond with one another (Tajeddin, Arabkhedri, 2020). Petrochemical polymers typically exhibit very good thermal and mechanical properties in the use of food packaging. Due to their economic availability, tensile strength, softness, and having a great barrier against aroma compounds and oxygen, synthetic polymers have been preferred as food packaging materials (Jabeen, Majid & Nayik, 2015). Polyethylene (PE), polyvinyl chloride (PVC), polyethylene terephthalate (PET), high-density polyethylene (HDPD), polystyrene (PS), and polypropylene (PP) are the ones that are used commonly in food packaging (Tajeddin & Arabkhedri, 2020).

Polyethylene (PE) is mainly used in industrial packaging applications due to its durability and ability to insulate and control vibration. PE is a closed-cell and light-weighted material (Berk, 2018). It comes in a number of different forms, including sheets, tubes, and pouches, and provides resistance against moisture and various chemicals (Sarmah & Rout, 2020). Although PE has advantages for food packaging, like other petroleum-based polymers it is harmful to the environment. The fact that most synthetic polymers are non-composable and nonbiodegradable has a significant negative effect on global warming and pollution. As a consequence, the packaging industry works to recycle and reuse packaging plastics in order to manage and control waste. For instance, PET has the ability to be recycled multiple times. In the USA approximately 681,000 tons of PET bottles are recycled every year (Clark, 2016). Since PET can be reused repeatedly, it is a very sustainable material.

Nevertheless, the environmental burden that comes from the nonrenewable nature of these polymers has increased the interest in the development of biodegradable polymers. Biodegradable polymers typically hydrolyze and decompose into carbon dioxide (CO_2), biomass, mineral mixes, or methane (CH_4) (Tajeddin, Arabkhedri,

2020). In the studies of Zhang et al. (2022), polyvinyl alcohol (PVA) was used to obtain a biodegradable active package by combining it with natural polymers. PVA is a water-soluble synthetic polymer with excellent mechanical, thermal, and optical qualities along with high transparency and low permeability to oxygen (Pereira et al., 2014). It has been approved by USDA for usage in poultry and meat packaging due to excellent properties such as biodegradability, nontoxicity and biocompatibility (Abdullah & Dong, 2019). Additionally, PVA also has outstanding bio-adhesive, emulsification, and film-forming capabilities together with great mechanical strength (Cai et al., 2016). PVA has excellent properties and also it has the advantage of being biodegradable, unlike most synthetic polymers. In the studies of Pereira et al. (2014), PVA was used in active film making by blending with chitosan. Indicator films having great physical and mechanical properties were successfully obtained with PVA. According to research that developed pH sensor films by using PVA combined with cellulose, PVA and cellulose-based films showed modified thermal and mechanical characteristics and biodegradability (Ding et al., 2020).

1.6.2. Biopolymers

The packaging industry is currently growing and has a significant impact on contemporary economies. Globalization, cutting-edge technologies, and rising consumer demands are just a few of the elements that have a significant impact on and fuel the growth of this industry. Food and drink comprise the greatest portion of this sector (85%), among other things (Bharimalla et al., 2017). Although it is commonly recognized that petroleum-based materials (such as polyethylene and polypropylene) have a detrimental effect on the environment, they are nonetheless frequently employed in the food packaging sector today. As a result, bio-based alternatives have enormous potential since they are biodegradable, do not harm the environment, do not cause cross-contamination during recycling, and pose no risk of toxicity to users (Ludwicka, Kaczmarek & Bialkowska, 2020). Growing awareness of the environmental problems and ecological imbalances brought on by the widespread use of environmentally unfriendly materials has sparked the creation of new natural, eco-friendly packaging alternatives. Despite their higher cost, bio-based

products have recently gained new attention due to the increased demand for eco-products on the market (Diez-Pascual, 2019). Both in the literature and on store shelves, various biopolymers can be discovered. In parallel, research on biopolymer alterations and modifications is driven by emerging trends in novel active and intelligent packaging development to create these eco-products with incredibly sophisticated features. One of these is bacterially produced nanocellulose (composites or native material), which has been employed as a natural bio-substrate for various applications, including medicine and cosmetics, but more recently, electronics and the packaging sector (Ludwicka, Kaczmarek & Bialkowska, 2020).

1.6.2.1. Bacterial Nanocellulose (BNC)

BNC is an exopolysaccharide that is straight and unbranched and is made up of extremely small nanofibrils. The small cross-section of the fibers in bacterial nanocellulose provides the high porosity of BNC. Gram-negative, aerobic bacteria of the *Komagataeibacter* genus are the primary, most effective, and extensively studied producers of BNC (Dima et al., 2017). BNC can be used for active and/or intelligent food packaging and edible food packaging. Food products should typically be protected chemically, biologically, and mechanically via biobased packaging. In this context, edibility, biodegradability, absence of toxicity, strong barrier, and high mechanical properties are the key benefits of using bionanocellulose in the food sector. BNC can be used widely as a secure food ingredient because it is a material that the US Food and Drug Administration (FDA) has classified as generally recognized as safe (GRAS) (Azeredo et al., 2019). The key advantage of this material among the other biopolymers is that the bacterial culture provides a full-size, reasonably thick membrane with excellent moldability and mechanical properties, which might be suitable for use in plain packaging material after purification and drying. However, there are some limitations in using native microbial cellulose, such as its hydrophilic nature or a lack of antibacterial and antioxidant activity of the membranes (Ludwicka, Kaczmarek & Bialkowska, 2020). BNC is continually being developed to overcome these restrictions. The most popular technique combines the inherent qualities of the BNC matrix with the physical, chemical, and biological

characteristics of different reinforcing compounds. This approach might enhance BNC parameters or produce microbial cellulose films with novel and desired properties required for certain applications (Azeredo et al., 2019).

To alter BNC and create an active or intelligent packaging material, a variety of additives may be used, such as stabilizers, plasticizers, oxygen scavengers, and antibacterial and antioxidative agents (Diblan, 2018). Through the immobilization of egg white lysozyme (Lys) on BNC matrices, Buruaga-Ramiro et al. (2020) created an active packaging material. BNC/Lys films were found to have antimicrobial activity towards Gram-positive and Gram-negative bacteria, according to experiments that were conducted. Additionally, studies into how these biocomposites perform in the packaging industry have shown that they can be kept at room temperature for a number of weeks without significantly losing their lysozyme activity (Buruaga-Ramiro et al., 2020). BNC/Lys membranes could therefore be used as a stable, environmentally friendly active packaging material. In order to create composites, Cabanas-Romero et al. (2020) submerged BNC in a chitosan solution. The created composite material demonstrated antioxidant activity, high mechanical qualities, and antibacterial activity against both Gram-positive and Gram-negative microorganisms.

In intelligent packaging, we use gas sensors to monitor food freshness by detecting the volatile components like amines, carbon dioxide, and oxygen that indicate food deterioration. For that purpose, Kuswandi et al. (2012) combined BNC and methyl red to develop an intelligent system that detects volatile amines released during food deterioration. One of the most recent advancements in the food packaging sector is the use of BNC intelligent packaging with a pH indicator. The essential components of freshness pH indicators are BNC support and a dye that reacts to changes in pH. An indicator relying on BNC and anthocyanins from black carrots was created by Moradi et al. (2019) This label was created by dipping BNC film into the anthocyanins solution. The colorimetric indicator demonstrated the capacity to recognize the pH increase that takes place as fish fillets degrade. Films that were red at pH 2 turned gray in alkaline settings when the pH rose due to food deterioration. Additionally, a colorimetric indicator was developed by Mohammadalinejhad et al.

(2020) to serve as a sensor for assessing the freshness of shrimp during refrigeration. The label was created using a BNC matrix and natural dye that was derived from *Echium amoenum* flowers. The study showed that the composite responded to pH fluctuations in the range of 2 to 12 by changing from purple to yellow, accordingly. Dirpan et al. (2018) provided another pH-sensitive indicator using a smart label made by dipping BNC films in a bromophenol blue solution. During application in packed mangoes, the color of synthetic pigment changed from dark blue to green in response to pH changes. Therefore, BNC has been used in many applications of active and intelligent food packaging by combining with different polymers, and functional.

1.6.2.2. Starch and Derivatives

Starch is a common natural polysaccharide. It has availability, renewable resource with favorable costs, and can increase the biodegradability of some materials that are blended with starch (Gonera and Cornillon, 2002). Starch coatings and films are mainly applied in the packaging of foods. Amylose and amylopectin are the macromolecules that compensate for each starch molecule. Amylose has a great ability to form tasteless, colorless, and odorless films. The ratio of amylose to amylopectin plays an important role in establishing the characteristics of starch and depends on the type of plant. Typically, starch includes 75-80% amylopectin and 20-25% amylose (Jimenez et al., 2012).

The mechanical properties of starch are poor and generally, it requires modifications or blending with other materials. Starch is plasticized by applying a certain amount of heat and mechanical energy in an extruder in order to use it as a thermoplastic material (Mangaraj, 2019). Thermoplastic starch blends, commonly referred to as starch plastics, can be used to package fruits and vegetables, or some dry goods in films, trays, and bags providing effective mechanical, oxygen, and moisture protection (Wesley et al., 2014).

1.6.2.3. Cellulose and Derivatives

The most widespread natural polymer is cellulose, which plays an essential structural role in plant cell walls (Sirviö et al., 2013). Wood is the primary source for cellulose synthesis by containing approximately 50% cellulose by mass. Cellulose is an edible and biodegradable polymer and is also widely known for qualities such as aroma, flavor, color, and taste. However, cellulose is not suitable for use in film-forming since it has a crystalline structure and insolubility in organic solvents and water. Thus, cellulose is transformed into cellophane which has outstanding barrier properties to oil and gas at low humidity and excellent mechanical characteristics but high moisture sensitivity. To enhance the barrier properties to moisture, cellophane is usually used with polyvinylidene dichloride (PVDC) or nitrocellulose wax (Kumar et al., 2011). In addition, cellulose can be processed into a number of commercially accessible derivatives, including microcrystalline cellulose (MCC), cellulose nanocrystals (CNC), cellulose acetate (CA), methylcellulose (MC), hydroxypropyl methylcellulose (HPMC), and carboxymethyl cellulose (CMC) (Liu et al., 2021). MCC and CNC are obtained by mechanical processes and acid hydrolysis of natural cellulose (Trache et al., 2016). Water-soluble derivatives of cellulose such as MC, HPMC, and CMC are prepared by using etherification reactions (He et al., 2020). In general, films made of cellulose variants are strong, flexible, completely transparent, and extremely sensitive to the presence of water, yet resistant to fats and oils (Alavi et al., 2015).

In the literature, cellulose derivatives are widely used in food packaging applications. In a study by Boonsiriwit et al. (2021), a sustainable intelligent package was successfully obtained by using MCC and HPMC. MCC is also used in biodegradable active packaging applications combined with starch and polylactic acid (Kale & Gorade, 2018; Cheng et al., 2021). Recently, there are also studies that use MC and CMC for obtaining environment-friendly active and intelligent packages (Roy & Rhim, 2020; Kanatt & Makwana, 2020; Zhou et al., 2021).

1.6.2.4. Chitin and Chitosan

Chitin, which is found predominantly in the shells of insects and crustaceans such as shrimp, crab, and crawfish, is a common natural biopolymer. Additionally, chitin can be formed by fungi and is found naturally in the cell walls of some fungi (Pokhrel, Yadav & Adhikari, 2015). The Chitin derivative which is chitosan can be formed by the deacetylation reaction of chitin. The insolubility of chitosan in water and alkaline mediums is caused by its crystalline structure and intense hydrogen bondings (Arvanitoyannis, 2014). Biodegradable and non-toxic chitosan can form strong, flexible, and clear films with great barrier properties. Chitosan is a desirable polymer for food packaging applications as it exhibits antibacterial activity against foodborne pathogens and spoilers (Santos et al., 2020). Low stability and weak water vapor barrier capabilities are the main drawbacks of chitosan.

1.6.2.5. Polylactic Acid (PLA)

Polylactic acid (PLA) is a recyclable biopolymer that is synthesized by lactic acid monomers. PLA is frequently included in blends, such as Ecovio, a PLA composite for food packaging that has previously received approval (Molenveld et al., 2015). With several uses as packaging bottles, barrier films, trays, and thermoformed items among others, PLA and PLA blends provide a great bio-based substitute for fossil plastics. Fruits and vegetables, which do not need a specific gas barrier and are packaged in atmospheric circumstances, are excellent examples of products with short shelf lives that benefit greatly from PLA packaging (Ramos et al., 2018). PLA can be blended with starch to create films, thermoformed hard plastic containers, foam, and trays. However, the release of additives from starch blends restricts their uses in contact with food (Molenveld et al., 2015).

1.6.2.6. Polyhydroxyalkanoates (PHAS)

Polyhydroxyalkanoates (PHA) are created naturally by bacteria fermenting lipids and sugar. Relying on the monomer utilized in the synthesis, they can be either thermoplastic or elastomeric materials with a melting point around 40 °C and 180 °C. Excellent packaging films can be produced using only these polymers or in blending with synthetic polymers or starches (Tharanathan, 2003). The most prevalent variety is polyhydroxybutyrate (PHB), which is produced when 3-hydroxybutyrate monomer is polymerized. PHB has qualities comparable to PP but is more rigid and also brittle. Polyhydroxybutyrate-Valerate (PHBV), a copolymer used in packaging applications, is less rigid and more durable (Siracusa et al., 2008). Although it is costly, it breaks down in 5–6 weeks in situations where microorganisms are active, producing water and carbon dioxide under aerobic conditions. Methane is produced more quickly during decomposition in an anaerobic environment. Yu, Chua, Huang, Lo, and Chen (1998) produced a variety of different PHA polymers having various physical and mechanical properties, such as flexibility, melting viscosity, and tensile strength, using food waste as the carbon source.

1.7. Metal-Organic Frameworks

Due to their consistent pore size and simplicity in functional customization, microporous polymeric materials have received a lot of interest in the previous two decades regarding their synthesis, characteristics, and wide range of applications. One of the most researched classes of extremely crystalline nanoporous materials is metal-organic frameworks (MOFs), sometimes known as hybrids of organic and inorganic. MOFs are made of coordinated organic ligands and three-dimensional crystalline porous networks of metal ions or clusters (Chirra et al., 2021). Figure 1.1 shows the formation of two- and three-dimensional MOFs. In order to promote oriented growth, a bottom-up method is frequently used to synthesize MOF structures. In this method, metal and organic molecules are induced to interact directly in a variety of synthesis

circumstances such as hydrothermal, mechanochemical, electrochemical, and sonochemical (Zhou, Long & Yagni, 2012).

MOF crystals have varied crystal structures (e.g., cubic, monoclinic, triclinic, orthorhombic, trigonal, tetragonal, and hexagonal) based on the metal ions and organic ligands chosen together with the synthesis conditions employed (Cheng et al., 2021). MOFs present a wide range of potential applications in the areas of gas separation and sorption, molecular sensing, biosensing, drug delivery, and chemical separations because of their excellent properties such as high surface area, nano-sized cavities, high stability, chemical tunability, ultrahigh porosity and crystallinity (Cravillion et al., 2009).

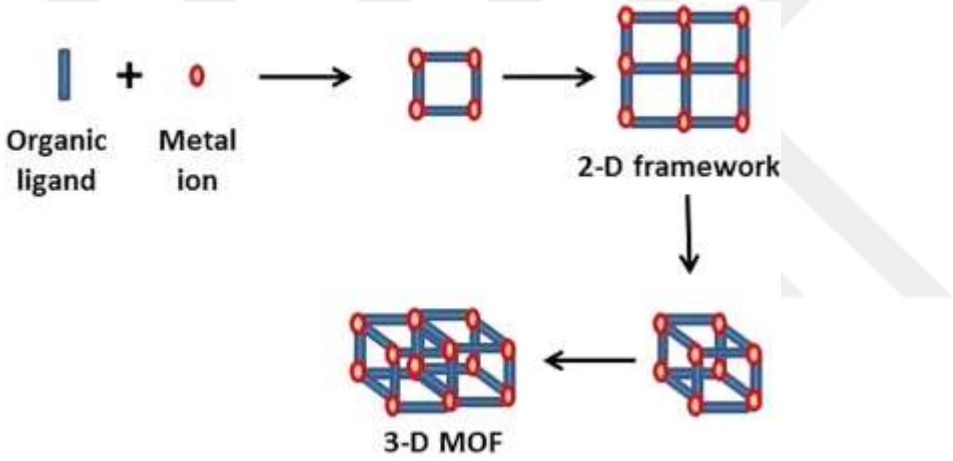

Figure 1. 1 Formation of MOFs.

MOFs are used in food applications as active contact materials, nanocarriers of active compounds and antimicrobial agents, and nanofillers of food packaging materials (Magri, Petriccione Gutierrez, 2021). Chopra et al. (2017) used different kinds of MOFs that are Zeolite Z13X, Basolite C300, and Basolite A520 as ethylene scavengers to extend the shelf life of banana. The study showed that MOFs are effective ethylene absorbers. Moreover, MOFs are recently used in carrying and controlled release of agents. For instance, in the study of Ma et al., (2020), a controlled release of curcumin in 3 hours is achieved by using curcumin carrying UiO-66. Wang et al. (2016) observed a comparable pattern in their analysis of allyl

isothiocyanate-loaded MOFs with 27 % load and retention of approximately two days.

A subclass of nanoporous MOFs known as zeolitic imidazolate frameworks (ZIFs) is similar to inorganic zeolites by having a sodalite structure and large pores (Kaur et al., 2017). Since the metal-organic framework hybrid structures of the ZIFs provide better adjustability in terms of design, functionality, and surface qualities, they are preferred over zeolites (Banerjee, 2009). Their chemical and thermal stability are excellent. ZIFs can be created using a straightforward, high-yield sol-gel process under standard settings, such as room temperature (Park et al., 2016). ZIFs are a fascinating subclass of crystalline microporous materials that exhibit unique and greatly desirable qualities shared by both ZIFs and MOFs. These characteristics include a great surface area with a large volume of micropores, accurate control of the size of pores, high crystallinity, homogeneous micropores, and high chemical and thermal stability (Chirra et al., 2021). Among the ZIFs, ZIF-8 has gained the most interest. 2-methylimidazole ligands and zinc metals are linked in the framework of ZIF-8, as illustrated in Figure 1.2. ZIF-8 has a cubic lattice and a faujasite zeolite topology is thermally stable up to 500 ºC, and has a high surface area, offering excellent sorption characteristics. All these properties make ZIF-8 as the most intriguing and extensively researched framework in the large ZIF family (Zheng et al., 2017). The use of ZIF-8 nanocrystals in food packaging applications increases from day to day. Nadar and Rathod (2020) used ZIF-8 as a stabilizer of enzymes. Protease and lipase enzymes have low physical and thermal stability, therefore ZIF-8 is used to stabilize them. In the study of Kim et al. (2021), ZIF-8 was used to coat surface-enhanced Raman scattering (SERS) paper while developing food spoilage detection. In addition, Wu et al. (2022) developed a nanoprobe to examine food spoilage by encapsulating doxorubicin into ZIF-8. In both of these studies, ZIF-8 nanocrystals provided great stability to the compound that is encapsulated and enhanced properties in thermal and surface characterizations.

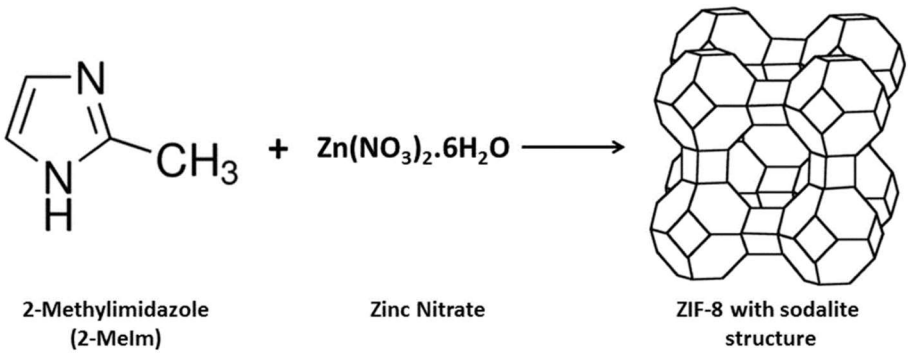

Figure 1. 2 Formation and structure of ZIF-8.

1.8. Objectives of the Study

Intelligent food packaging has various benefits, including the ability to detect and record the atmosphere in which the food is stored and to monitor the current freshness/spoilage status of the product. To indicate food spoilage, some compounds can give color responses when they are exposed to volatile substances like basic amines. Anthocyanins are one of the widely used natural coloring pigments in food freshness monitoring. They exhibit an excellent color change in exposure to different pH values. However, anthocyanins generally have low stability and poor mechanical and thermal characteristics. In order to use anthocyanins efficiently as pH-sensitive indicators, encapsulation can be used to improve poor qualities.

BNC is a widely used biopolymer in food packaging applications. For obtaining sustainable light-weighted, odorless, and tasteless intelligent or active films, BNC is very suitable. Although BNC has been used in a number of various applications such as gas sensor films, colorimetric films, and sustainable and edible films, the capability of BNC in the production of a multilayer intelligent film is not investigated. Therefore, using BNC sheets to obtain multilayer films is a novel approach for this study.

The applications of ZIFs in food packaging have increased recently. ZIFs offer many advantages such as enhanced mechanical properties, high porosity surface, and long-term stability. Using ZIFs as a carrier of anthocyanins can provide a more stable color

response in the colorimetric detection of food spoilage. Also, it is possible to obtain enhanced mechanical and surface specifications of colorimetric films.

While developing a colorimetric indicator material, it is important to use proper support compounds to improve mechanical and barrier properties. PVA is a commonly used non-toxic and biodegradable polymer in food applications. It also has great barrier characteristics, along with excellent film-forming ability. Therefore, the aims of this study were to develop a pH-sensitive multilayer colorimetric film using anthocyanins-loaded ZIF-8 nanocrystals through coating them with PVA into BNC sheets and evaluate the optical, morphological, thermal, and mechanical characteristics of these multilayer films with a different number of coating layers. The developed indicators were applied for monitoring freshness in skinless chicken breasts during storage at refrigerator conditions.

CHAPTER 2

MATERIAL AND METHOD

2.1. Materials

Red grapes (*Vitis vinifera*) and skinless chicken breast were purchased from a local market in Ankara (Turkey). Polyvinyl alcohol, 2-methylimidazole, zinc nitrate hexahydrate, methyl red and bromocresol green indicators, boric acid, sodium phosphate dibasic, sodium phosphate monobasic, plate count agar, and magnesium oxide were supplied by Sigma-Aldrich (St. Louis, MO, USA). Ammonium hydroxide (25%), ammonium chloride, hydrochloric acid fuming (37%), ethanol, and methanol were provided by ISOLAB (Wertheim, Germany). The nutrient broth was purchased from Merck (Darmstadt, Germany).

2.2. Synthesis and Characterizations of Anthocyanins, ZIF-8 and Anthocyanins Loaded ZIF-8 (GSE@ZIF-8)

2.2.1. Extraction of anthocyanins from red grape skin

Anthocyanins extraction from red grapes was carried out corresponding to a solvent-extraction technique described by Chandrasekhar et al., (2012). A 50 g sample of red grape skins was taken and introduced to 100 ml of methanol. Extraction was performed by stirring solid-liquid media at 500 rpm for 24 hours. The extract was filtrated initially with Whatman paper and then using a 0.45μm syringe filter. The pH differential method was used to determine the concentration of red grape anthocyanins (Lee et al., 2005). The stock solution of grape skin extract (GSE) was adjusted to 0.5 g/l in methanol.

2.2.2. Synthesis of ZIF-8 and GSE@ZIF-8

ZIF-8 synthesis was carried out according to the method of Tiwari et al (2017). A solution of 150 mg of $Zn(NO_3)_2.6H_2O$ was prepared in 5 ml deionized (DI) water. In the meantime, a second solution was prepared by adding 330 mg of 2-methylimidazole into 10 ml of GSE stock. After homogeneous solutions were obtained, the first solution rapidly poured into the second one. The final solution was stirred at 500 rpm for 1 hour. Grape skin extract loaded with ZIF-8 (GSE@ZIF-8) was obtained at the end of 1 hour and was washed three times with ethanol by centrifugation at 15000 rpm for 12 minutes. A similar protocol was followed for the synthesis of ZIF-8, and the only difference came from the content of the second solution, which was prepared by mixing 330 mg of 2-methylimidazole in 10 ml methanol without GSE. Subsequently, GSE@ZIF-8 and ZIF-8 nanocrystals were vacuum-dried before further analysis.

2.2.3. Optical Characterization of GSE, ZIF-8 and GSE@ZIF-8

UV-Vis spectra of GSE, ZIF-8, and GSE@ZIF-8 were monitored between 400-700 nm by using UV-Vis spectrophotometer (Optizen Pop, Mecasys, Seoul, Korea). The spectra of GSE (0.2 mg/ml) and GSE@ZIF-8 (0.5 mg/ml) were measured in 0.1 M sodium phosphate buffers in a range of pH 1 to 12. The spectral comparison of ZIF-8 and GSE@ZIF-8 was performed at a pH 2 buffer of sodium phosphate (0.1 M).

2.2.4. Surface, Structural and Thermal Characterizations of ZIF-8 and GSE@ZIF-8

Surface area and porosity characterization of ZIF-8 and GSE@ZIF-8 were determined by BET analyzer (AUTOSORB-6B) with the single point analysis of BET. High-resolution electron microscopy (HRTEM) (FEI, Tecnai G2 Spirit

Biotwin, Oregon, USA) was used to measure the morphological properties of ZIF-8 samples. Chemical bond and structural characteristics of GSE, ZIF-8, and GSE@ZIF-8 were detected by Fourier transform infrared spectroscopy (FTIR) (SHIMADZU, IRSpirit, Kyoto, Japan). The range of spectrum was 4000-500 cm^{-1} at a resolution of 4 cm^{-1}. X-Ray Diffractometer (XRD) was used to examine the crystallinity of ZIF-8 and GSE@ZIF-8 in the range of 5º to 50º. Thermogravimetric analyzer (TGA) and differential scanning calorimeter (DSC) (TA instruments SDT 650 Simultane DSC/TGA) were used for the determination of thermal characteristics of GSE, ZIF-8, and GSE@ZIF-8. The heating rate was 10 ºC/min, and the range was 2 5ºC to 600 ºC.

2.3. Fabrication and Characterization of Multilayer Films

2.3.1. Synthesis of BNC

To synthesize BNC membrane, Komagataeibacter xylinus subsp. sucrofermentants was used utilizing an optimized procedure under a static culture environment with citric acid, disodium hydrogen phosphate, molasses, gluten, ammonium sulfate and ethanol at specified concentrations (Moradi et al, 2022). After three days of inoculation the wet membrane of BNC was obtained. Then, synthesized BNC was washed to neutralize pH and decolorized. Finally, dried BNC sheets were obtained by air drying at 40 °C for 2 days.

2.3.2. Fabrication of Multilayer Films

The films were fabricated by the spin coating method. Firstly, PVA was dissolved in DI water by continuous mixing at 90 ºC for 4 hours to obtain an 8%(w/v) solution. Then, the PVA solution is mixed with 40 mg/ml of GSE@ZIF-8 in DI water by ultrasonication for 10 minutes. The final mixture contained 20 mg/ml of GSE@ZIF-8 and 4%(w/v) PVA in DI water. Secondly, BNC sheets were cut into (2 cm x 2 cm) pieces. 200 µl of the prepared mixture was coated on the pieces of BNC by a spin

coater (VTC-200 Vacuum Spin Coater, Shenyang Kejing, China) at 500 rpm for 60 seconds. After coating, the films were dried at 40 ºC. Samples with a varying number of coating cycles (1, 2, and 3 cycles) were obtained and labeled as BNC-1PVA/GSE@ZIF-8, BNC-2PVA/GSE@ZIF-8 and as BNC-3PVA/GSE@ZIF-8. The colorimetric films were conditioned in a climate chamber at 50% relative humidity and 20ºC before analysis.

2.3.3. Mechanical and barrier characterization of colorimetric films

Water vapor permeability (WVP) was measured by a method described by McHugh et al. After measuring the thickness of the samples at 7 different locations using a micrometer (LOYKA 5202-25, Ankara, Turkey), 35 ml of water was poured into cylindrical water vapor permeability test cups with an inner diameter of 4 cm to obtain 100% relative humidity. Then, the films were placed between the cup and the cover. The cups were weighted initially and placed into a desiccator. The weight changes of cups, temperature and relative humidity values of the surrounding environment were monitored every hour for 10 hours. The WVP values were reported as g/m.s.Pa.

2.3.4. Moisture Content and Water Solubility of the Films

To determine the moisture content, films with the size of 2 cm × 2 cm were prepared and weighted (W_0). Then, films were dried at 105 ºC till constant weight (W_1) was obtained. Moisture content was decided by Eq. 1.

$$\%MC = \frac{W_0 - W_1}{W_1} \times 100 \qquad (1)$$

To determine water solubility , films with the size of 2 cm × 2 cm were added and stirred in beakers filled with 50 mL distilled water for 24 hours at 23ºC. Then, the insoluble residues of the films were separated from water by filter paper and dried

at 105 ºC until the constant weight (W_2) was obtained. Determination of water solubility was performed using Eq. 2.

$$WS = \frac{W_0\left(1-\%\frac{MC}{100}\right)-W_2}{W_0\left(1-\%\frac{MC}{100}\right)} \times 100 \qquad (2)$$

2.3.5. Thermal and Morphological Characterization of Multilayer Films

Thermal properties of the colorimetric films were measured by a differential scanning calorimeter (Perkin Elmer, DSC 4000, CT, USA). Samples dried in a vacuum-dryer at 40 °C were sealed into aluminum pans (5g) after weighing. Scanning was carried out under inert nitrogen gas in the temperature range of 25 ºC – 250 ºC with a heating rate of 10 ºC/min. An empty sealed pan was taken as a reference sample. A field emission scanning electron microscope (FESEM) (FEI, QUANTA 400F Field Emission SEM, Oregon, USA) was used for the cross-sectional analysis of multilayer films. An accelerating voltage of 10 kV was applied to the film samples, which were cryofractured and placed onto the aluminum stubs.

2.3.6. Color Response of the Films to Volatile Ammonia

The color response of the films was determined by exposing films to different ammonia concentration solutions. Firstly, a stock solution of ammonium chloride and concentrated ammonia (1 M) was prepared. Then, 2 cm × 2 cm films were placed 1 cm above the 20 mL of ammonia solution in a beaker. Gaseous ammonia concentration was estimated based on 'Raoult's law by using the partial vapor pressure of ammonia at 23 ºC and the initial ammonia concentration in a 20 mL solution. A determined amount of stock solution was injected to obtain *in situ* ammonia gas concentrations as 3, 7, 15, 30, 60, and 120 mg N/100 g, and DI water was taken as a reference of 0 mg N/100 g at 23ºC. After 24 hours of exposure to different concentrations of volatile ammonia, images were captured using a smartphone (LG,

G6, Yeouido-dong, Seoul, South Korea) with a custom-made 3D holder to minimize the background light exposure. ΔE values were calculated based on Eq. 4. L^* values correspond to lightness, while a^* values correspond to colors from red to green and b^* values are from yellow to blue. ImageJ program was used to extract L^*, a^*, and b^* values from the taken images.

$$\Delta E = \sqrt{(L_0^* - L^*)^2 + (a_0^* - a^*)^2 + (b_0^* - b^*)^2} \qquad (4)$$

2.3.7. Chicken Spoilage Trials

Ten grams of skinless chicken breast samples were placed in the sterilized polystyrene foam containers (5 cm in height). The film of 2 cm × 2 cm was first attached to the cellophane and then located 1 cm above chicken samples by sealing the top of the foam container with cellophane. The containers with samples were stored for 10 days at 4 ºC. Day-by-day color changes were monitored by taking images of the films with a smartphone as described in Section 2.3.5.

2.3.8. TVB-N Measurements of Chicken Samples

For TVB-N measurements, 10 g of chicken samples were homogenized with 100 mL distilled water for 2 minutes using the stomacher (Wisd, WES-400 model). Homogenized mixtures were centrifugated at 10000 rpm for 12 minutes. The corresponding supernatant was collected and added to an equal volume of 1 % (w/v) MgO solution. Steam distillation was performed, and the distillate was collected in a flask with 25 mL of boric acid (20g/l) and methyl red-bromocresol green indicator. After distillation, the obtained mixture was titrated with 0.01 M HCl solution till the color pink was observed. TVB-N was calculated by using Eq 5.

$$TVB - N = \frac{(V_1 - V_0)x0.14x1x100}{M} \qquad (5)$$

Where M(g) is the weight of the sample, V_1(mL) and V_2(mL) are the volumes of titration of the sample and blank.

2.3.9. Microbiological analysis

Ten grams of chicken breast sample was mixed with 100 mL of sterile peptone water in a sterile bag and homogenized in the stomacher (Wisd, WES- 400 model) for 2 minutes. A series of dilutions were carried out according to microbiological protocols. 100 µL of each diluted sample was planted on agar, which is prepared by plate count agar, plates using the spread plate method. After incubation at 37 ◦C for 48 hours, colony-forming units were counted and recorded as cfu/g.

2.4. Statistical Analysis

All of the experiments were performed in triplicate. Statistical analysis was carried out by using MINITAB (version 16). One way of variance was performed with Tukey's multiple comparison tests for analysis of experimental data.

CHAPTER 3

RESULTS AND DISCUSSIONS

3.1. Optical Characterizations of GSE

The colorimetric indicators monitor the condition of the food products and show color change with perishing. Hence, anthocyanins containing indicator films are able to detect food spoilage. Anthocyanins provide a rapid and reversible change in a wide spectrum of color when the hydroxyl groups of phenolic compounds on the structure of anthocyanins are protonated or deprotonated (Prietto et al., 2017). Especially in protein-rich foods, total volatile amines are released as food begins to deteriorate and these volatile amines cause the color change of anthocyanins. The color response of GSE along the varying pH values from pH 1 to pH 12 is demonstrated together with images of GSE solutions in Figure 3.1. As indicated, at lower ph values such as pH 1 to 4, reddish colors were observed, while the color slowly changed into purple with the increasing pH values between pH 4 and 7. When pH levels rose over 7, the color was observed as blue and its shades up to pH 9, and then the color altered to green at the values from pH 9 to 11. Finally, the color of GSE solution was yellow at a pH of 12, the highest pH value tested. UV-Vis spectrum in the range of 400 nm to 700 nm of RSE is shown in Figure 3.1. For pH values between 1 and 5, the maximum absorption peak was observed at 520 nm, and the peak intensity gradually reduced through pH 1 to 7 due to the hypochromic and bathochromic effects caused by the reaction of flavylium cations (Cruz et al., 2022). As evidenced in the GSE spectra, the highest absorption peak at 600 nm was present at pH 10, and the intensity of this peak decreased from pH 10 to pH 12. Correspondingly, the colorimetric characteristics and the spectrum of GSE were consistent with the studies conducted on red grape anthocyanins in the literature (Alizadeh-Sani et al., 2020; Merz et al., 2020).

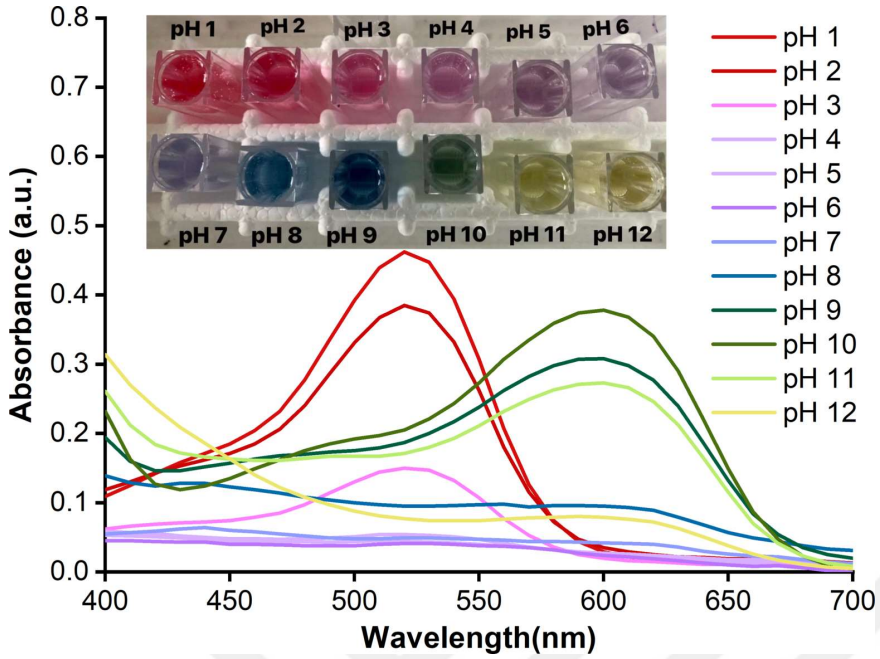

Figure 3. 1 UV-Vis spectra of GSE and inserted image of observed color changes in different pH values

3.2. Characterization of ZIF-8 and GSE@ZIF-8

3.2.1. Optical Characterizations of ZIF-8 and GSE@ZIF-8

Figure 3.2a. shows the absorbance spectra of GSE@ZIF-8 solution in different pH values. As seen, the absorption spectra of GSE@ZIF-8 matched the spectra of GSE. Figure 3.2b. indicates the absorbance spectra of ZIF-8 and GSE@ZIF-8 in pH 2 buffer solution. There was no detectable characteristic ZIF-8 absorbance peak within the studied range of 400 to 700 nm in UV-Vis spectra. According to the study on curcumin encapsulation in ZIF-8, the UV-Visible spectra of ZIF-8 also did not exhibit any particular peak corresponding to ZIF-8 (Tiwari, Singh, Garg & Randhawa, 2017). On the other hand, GSE@ZIF-8 displayed a significant peak positioned around 520 nm wavelength, which indicates that encapsulation of anthocyanins in ZIF-8 molecules was successfully performed. The formation of intramolecular hydrogen

bonds within the phenolic groups and the nitrogen atoms might lead to the encapsulation of the anthocyanin into the ZIF-8 framework (Liedana et al., 2012)

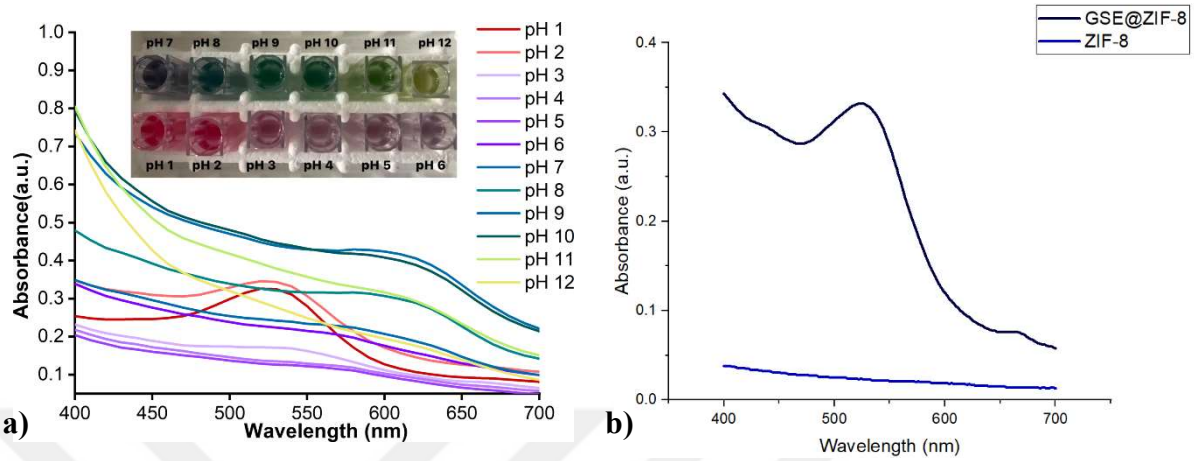

Figure 3. 2 (a) UV-Vis spectra of GSE@ZIF-8 at pH range of 1-12 and visible color change in inserted image. (b) UV-Vis spectra of ZIF-8 and GSE@ZIF-8 in pH 2 sodium buffer.

3.2.2. Structural Characterizations of ZIF-8 and GSE@ZIF-8

The morphological characterization of GSE@ZIF-8 was performed by using TEM. The GSE@ZIF-8 images displayed rhombic dodecahedron-shaped ZIF-8 particles with an average crystal size of 50 nm. Obtained morphologic characteristics for ZIF-8 were in line with the literature (Tiwari et al., 2017). XRD was used to analyze the crystallinity and phase purity of ZIF-8 and GSE@ZIF-8. XRF patterns of ZIF-8 were illustrated in Figure 3.3b. The positions and characteristic peaks in XRD patterns of ZIF-8 closely matched those in the literature (Nordin et al., 2017). When compared to ZIF-8, the XRD pattern of GSE@ZIF-8 was remarkably similar to that of ZIF-8. They both showed the same characteristic peaks at 2θ approximate values of 7.3, 10.4, 12.8, and 18.1°, respectively corresponding to index planes of (110), (200), (211) and (222) (Tiwari et al., 2017).

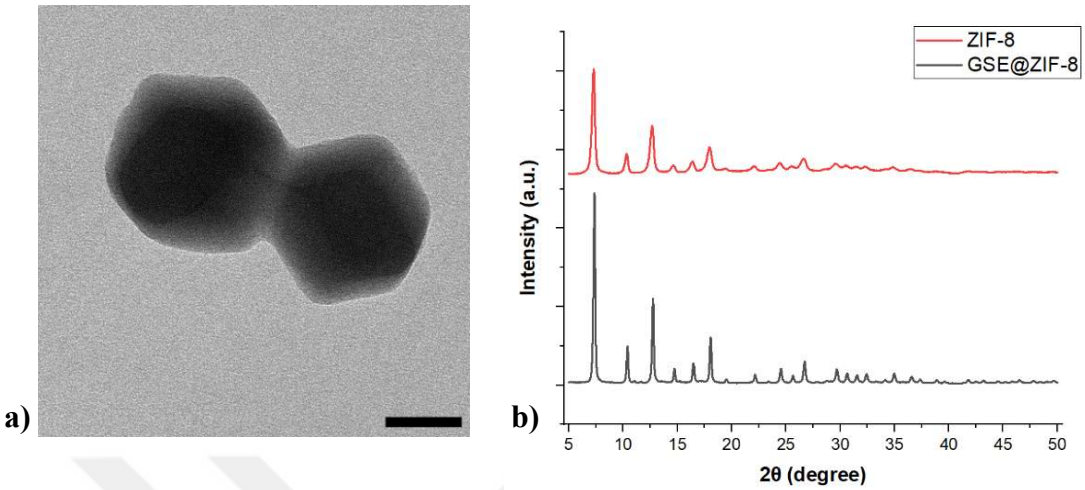

Figure 3. 3 (a) TEM image of GSE@ZIF-8 (50 nm scale). (b) XRD patterns of ZIF-8 and GSE@ZIF-8

BET adsorption tests were conducted to investigate the porosity and surface area of ZIF-8 and GSE@ZIF-8. BET isotherms emphasize adsorption isotherms at very low relative pressure in Figure 3.4a. A considerable increase in nitrogen uptake throughout adsorption studies at low relative pressures verified the microporosity of ZIF-8 and GSE@ZIF-8. In addition, the BET surface area of ZIF-8 and GSE@ZIF-8 was determined to be 1661 m^2/g and 1118 m^2/g, respectively. The fact that GSE@ZIF-8 had a lower surface area in comparison to ZIF-8 demonstrated the efficient encapsulation of GSE in ZIF-8 frameworks. Loading of GSE resulted in a pore size reduction of the frameworks. However, in general, the pore size distributions stayed similar as illustrated in Fig 3.4b.

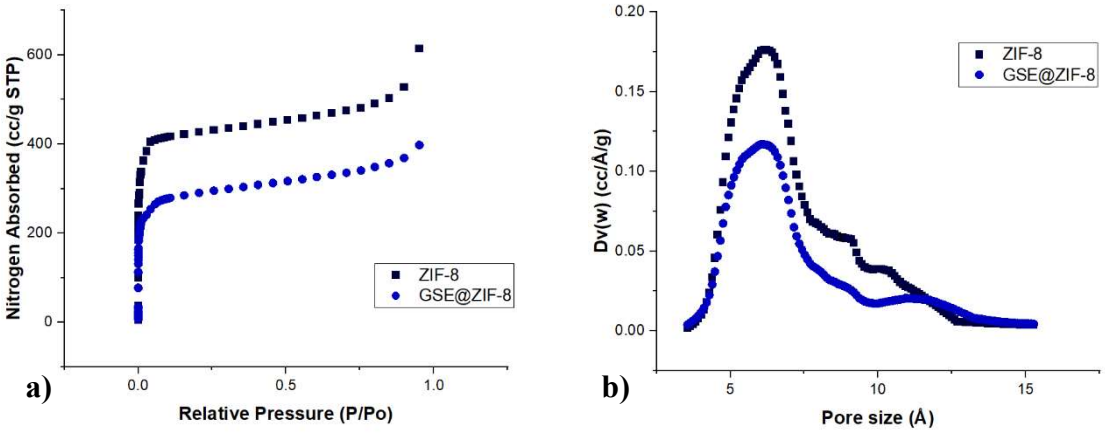

Figure 3. 4 **(a)** Nitrogen sorption isotherms and**, (b)** pore size distributions of ZIF-8 and GSE@ZIF-8

FTIR spectra of GSE, ZIF-8 and GSE@ZIF-8 are given in Fig 3.5. The FTIR spectra give detailed information on how chemical bonds interact and change. For ZIF-8, characteristic peaks were detected at around 1605 cm^{-1} and 1500 cm^{-1} corresponding to C-C stretching and vibrations of C=C stretching. Furthermore, C-N stretching can be observed at approximately 1310 cm^{-1} and 1150 cm^{-1}. The peaks observed around 760 cm^{-1} and 690 cm^{-1} were attributed to the vibrations of Zn-O and Zn-N stretchings. Besides these, the FTIR analysis of GSE revealed a hydroxyl peak at 3265 cm^{-1} and vibrations of aromatic C-H stretching at around 2920 cm^{-1} (Gokilamani et al., 2013). The stretching vibration peak that occurred at 2360 cm^{-1} could be caused by the flavylium cation of GSE at the B ring, whereas the peak at 1595 cm^{-1} was ascribed to C=C stretching of the benzopyran ring. Additionally, the peak appearing around 1030 cm^{-1} was attributed to flavonoid compounds of the aromatic ring (Ramamoorthy et al., 2016). When investigating the FTIR spectrum of GSE@ZIF-8, the majority of the typical peaks of ZIF-8 and GSE matched. However, the spectrum of GSE@ZIF-8 showed two more unique peaks, which were different from that of ZIF-8. The C-O angular deformation of phenols may be responsible for the peak that appeared at 1380 cm^{-1}, whereas the stretching vibrations of aromatic rings of anthocyanins could be accountable for the peak that arose at around 950 cm^{-1}.

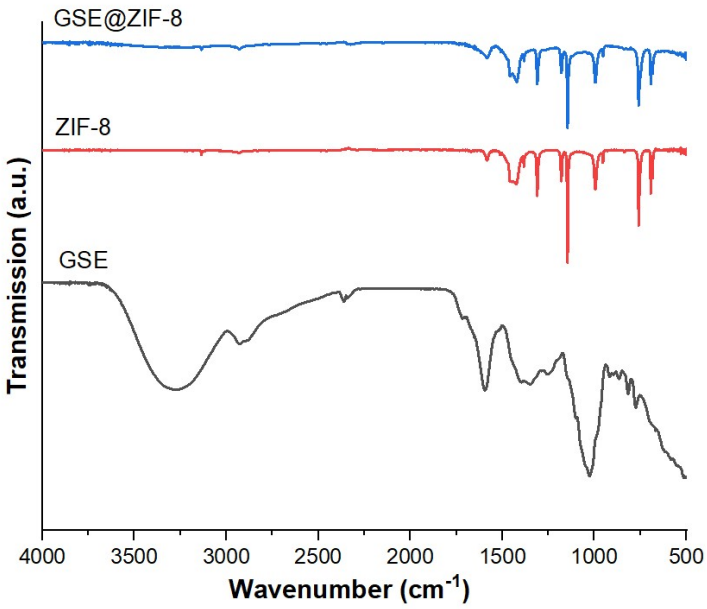

Figure 3. 5 FTIR spectra of GSE, ZIF-8 and GSE@ZIF-8

3.2.3. Thermal Characterizations of ZIF-8 and GSE@ZIF-8

TGA is a technique for assessing thermal stability and the proportion of volatile components by analyzing weight changes that occurred during constant rate heating. The TGA and DTG (derivative thermogravimetry) analysis results of GSE, ZIF-8, and GSE@ZIF-8 are demonstrated in Fig 3.6. Initially, weight loss was monitored for all samples at around 100 ºC, which might be attributed to a minor quantity of unbound water. GSE underwent the second degradation step at about 150 °C, which might be ascribed to the formation of volatile phenolic acids and aldehydes from ring-opening reactions of anthocyanins (Silva et al., 2019). For ZIF-8, there was no noticeable change occurring at the range from 120 °C to 600 °C, which confirms the excellent thermal stability of ZIF-8 nanocrystals. Further, the weight loss at around 600 °C might indicate that ZIF-8 was entirely decomposed. The thermal stability of ZIF-8 was found to be similar to as reported in the literature (Tran, Le & Phan, 2011). In TGA results of GSE@ZIF-8, the initial loss of weight observed between 250 °C and 300 °C was attributed to the thermal degradation of GSE. However, after being encapsulated into the ZIF-8 framework, the weight loss significantly decreased. That means encapsulating GSE into ZIF-8 improved the thermal properties. In other

words, encapsulated GSE showed better thermal stability than normal GSE. Overall, the results supported that GSE is successfully encapsulated into ZIF-8 and thermal stability was enhanced after encapsulation.

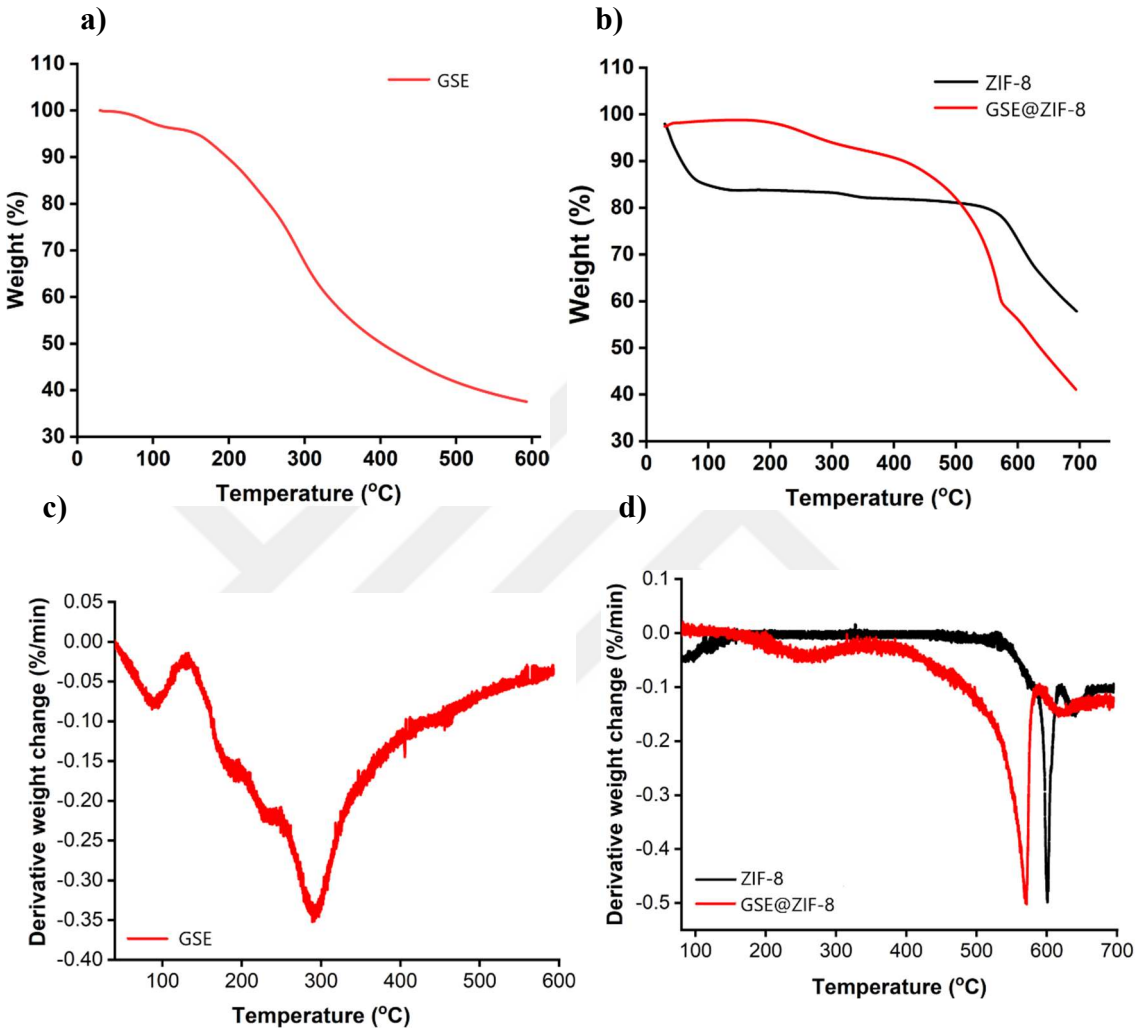

Figure 3. 6 **(a)** TGA curve of GSE, **(b)** TGA curve of ZIF-8 and GSE@ZIF-8 **(c)** DTG curve of GSE **(d)** DTG curve of ZIF-8 and GSE@ZIF-8

3.3. Characterization of Multilayer Films

3.3.1. Thermal Characterization of Films

DSC was used to analyze the thermal properties of multilayer colorimetric films. Table 3.1 shows peak temperatures and enthalpies of all the compounds and films obtained from DSC. Two endothermic peaks of PVA were observed at 86.9 °C and 228.5 °C, which were in line with the literature (Gupta, 2009). The second

temperature was ascribed to the melting of PVA crystals. Similar to PVA, DSC results of BNC also greatly complied with other studies in the literature by having a characteristic peak of melting of the crystalline phase temperature at 126 °C (Pa'e et al., 2018). Moreover, the anthocyanins underwent thermal deterioration, which was detected with an endothermic peak at around 156.7 °C. In the literature, the endothermic breakdown peak of anthocyanins was shown to be approximately at the same temperature range (Silva et al., 2019). All three multilayer films were shown two peaks at similar temperature ranges of 135-140 °C and 216-228 °C. The higher peak temperature might be attributed to more stable encapsulated anthocyanins in ZIF-8 whereas the presence of PVA and BNC could be responsible for the lower peak temperatures. The results obtained by DSC comply well with the TGA results of GSE and GSE@ZIF-8.

Table 3. 1 DSC analysis of grape skin extracts, bacterial nanocellulose, polyvinyl alcohol and films with changing numbers of layers

		T (ºC)	**ΔH (J/g)**
Anthocyanins	Peak 1	156.7	133.81
	Peak 2	-	-
BNC	Peak 1	126.1	53.19
	Peak 2	-	-
PVA	Peak 1	86.9	24.245
	Peak 2	228.5	61.82
BNC-1PVA/GSE@ZIF-8	Peak 1	140.24	14.08
	Peak 2	222.55	7.35
BNC-2PVA/GSE@ZIF-8	Peak 1	135.07	27.8
	Peak 2	216.56	17.28
BNC-3PVA/GSE@ZIF-8	Peak 1	139.02	34.01
	Peak 2	219.5	17.79

3.3.2. Water Solubility and Barrier Characterizations of Multilayer Films

The WS value of the films shows the water resistance of the films that affect the barrier characteristics of films. Table 3.2 shows the WS values of multilayer films and control BNC films. Among the tested films, BNC demonstrated the greatest resistance to water with a solubility value of 8%. The low solubility of BNC originates from intense intermolecular and intramolecular hydrogen bonding of cellulose chains (Heise et al., 2020). Additionally, WS significantly increased with the increasing number of PVA/A-ZIF-8 layers on BNC. The high polarity hydroxyl groups on the PVA structure might be the main reason for the increase in the WS in BNC-PVA/A-ZIF-8 films (Brough et al., 2016)

Table 3. 2 Water solubility, thickness and water permeability of the films

Film	**WS (%)**	**Thickness (mm)**	**WVP ($x10^{-11}$ g m^{-1} s^{-1} Pa^{-1})**
BNC	7.93 ± 3.89^{a}	0.013 ± 0.001^{a}	5.33 ± 0.27^{a}
BNC-1PVA/GSE@ZIF-8	18.45 ± 5.71^{ab}	0.017 ± 0.003^{a}	6.81 ± 0.80^{b}
BNC-2PVA/GSE@ZIF-8	28.53 ± 4.50^{bc}	0.026 ± 0.003^{b}	9.96 ± 0.55^{c}
BNC-3PVA/GSE@ZIF-8	30.94 ± 4.61^{c}	0.031 ± 0.002^{b}	10.80 ± 0.38^{c}

WVP is a critical attribute for applications of food packaging since the transfer of water vapor through the package increases the possibility of food spoilage and quality deterioration. The film thickness should be carefully considered in WVP measurements because there is a positive correlation between film thickness and WVP (Bertuzzi, Vidaurre, Armada & Gottifredi, 2016). As seen in Table 3.2, the WVP values substantially increased with the number of layers and, consequently, led to an increase in the thickness of the films. The increase in WVP values of the films could be explained by the hydrophilic nature and, thereby, the greater water permeability of PVA than BNC. Besides, metal-organic frameworks (MOFs) with

high porosity were effective in enhancing of WVP since molecules can be efficiently transferred through the hydrophobic channels of MOFs. In this case, ZIF-8 molecules had an impact on the increase WVP due to their porous structure. Similar results were obtained in the literature that studied BNC and modified BNC films (Cazon & Vasquez, 2021). Generally, biopolymers display greater permeability to water vapor (Silva et al., 2020).). However, the PVA/GSE@ZIF-8 layer deposition resulted in an unfavorable increase in the WVP of multilayer BNC films.

3.3.3. Microstructural Analysis of Colorimetric Films

FESEM was used to investigate the cross-sectional morphological characteristics of the films. The entangled fiber network of BNC was visible in the FESEM images of uncoated BNC as predicted in Figure 3.7. As the PVA/GSE@ZIF-8 layer was coated on BNC, the surface of the multilayer films was observed to be smoother and also more compact. The crossectional images of the films showed homogeneous, consistent microstructures without any delamination. On the BNC network, an increase in the thickness of PVA/GSE@ZIF-8 layer with the number of coating cycles was also clearly visible.

a) b)

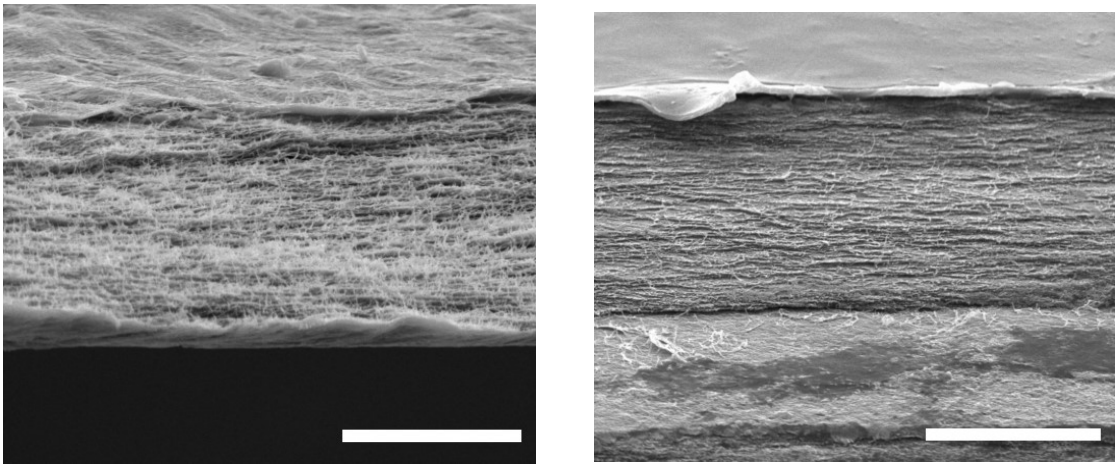

c) d)

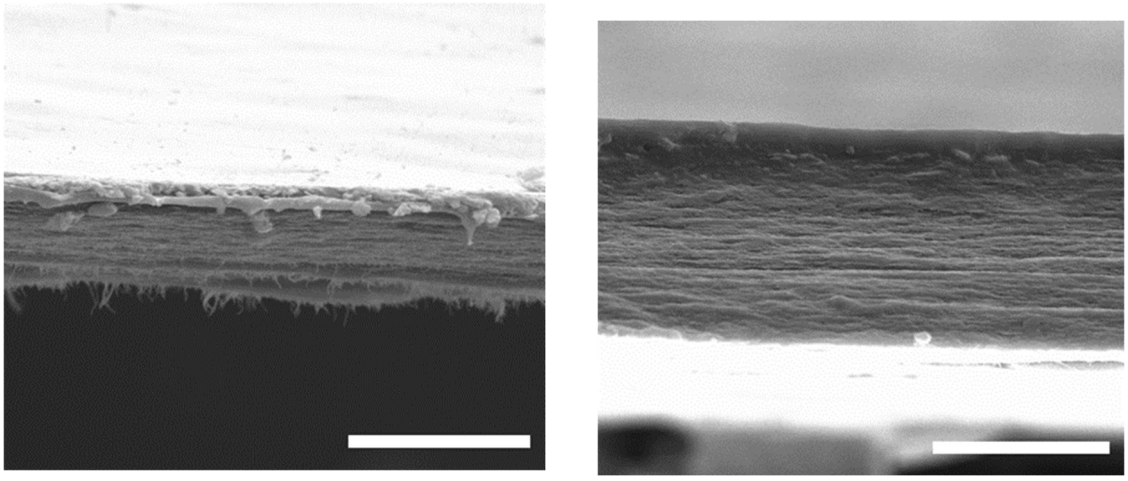

Figure 3. 7 FESEM cross-sectional images (10 µm scale bar) of BNC and films with different numbers of layers

3.3.4. Colorimetric Analysis of Multilayer Films

The formation of basic amines such as ammonia, trimetyhlamines, and dimethylamines results from the decarboxylation of enzymatic amino acids caused by microbial enzymes and tissue activities in protein-rich food (Zhang et al., 2019). Ammonia has the lower boiling point among the three TVB-N molecules (ammonia, di- and trimethylamines) that are most frequently produced during spoilage. As a result, to simulate TVB-N molecules, which are responsible for the sensory detection of food deterioration, ammonia was chosen (Liu, Cui, Shang & Zhong, 2021). The color responses of multilayer films to various ammonia concentrations are shown in Tables 3.3, 3.4, and 3.5 with the corresponding values of L^*, a^*, b^*, and ΔE. Color of BNC-1PVA/GSE@ZIF-8 were turned into blue from purple upon exposure to 7 mg N/100 g ammonia concentration (Table 3.3). Accordingly, a significant change was observed in the a^* value of the film. Nevertheless, no significant difference was seen in other tested ammonia concentrations at a critical concentration of ammonia, which is 30 mg/100 g for poultry. BNC-1PVA/GSE@ZIF-8 had higher sensitivity to ammonia. Therefore, films with a single layer of PVA/GSE@ZIF-8 coating were not acceptable for monitoring chicken spoilage since the critical value of the TVB-N level was set to be 30 g/ 100 g in the Turkish Standards (TS 24019, 2014).

Table 3. 3 Color response to ammonia results of single-layered film

Ammonia concentration (mg/100 g)	Film images	*L**	*a**	*b**	ΔE
0		53.75±2.50^{a}	11.75±0.96^{a}	-3.50±1.00^{a}	-
3		52.25±3.20^{a}	10.00±1.41^{a}	-3.00±0.00^{a}	3.95±0.66^{a}
7		60.75±2.06^{a}	-5.00±0.82^{b}	-8.00±1.41^{b}	17.33±0.69^{b}
15		57.25±5.32^{a}	-12.00±1.83^{c}	-8.00±3.27^{b}	23.66±1.88^{c}
30		58.50±4.65^{a}	-15.25±2.22^{cd}	-5.50±1.29^{ab}	26.37±1.90^{cd}
60		55.00±4.32^{a}	-17.00±2.16^{d}	-8.00±2.58^{b}	28.16±2.05^{d}
120		59.75±4.57^{a}	-16.00±2.71^{cd}	-4.00±0.81^{ab}	27.19±2.43^{cd}

In Table 3.4, the color response of BNC-2PVA/GSE@ZIF-8 films was illustrated. A significant color change was observed at around 30 mg N/ 100 g ammonia concentration. Before that, the color of the films was reddish purple and the color turned into blue at 30 mg N/ 100 g. Then it gradually became green with an increasing concentration of ammonia. The *a** value of BNC-2PVA/GSE@ZIF-8 steadily and significantly reduced starting at the concentration of 15 mg N/100 g. That result supported the color response of the films because the change of *a** value from positive to negative indicates the color change from red to green. Besides, ΔE values changed significantly after 15 mg N/ 100 g concentration of ammonia. Regarding these results, BNC-2PVA/GSE@ZIF-8 films worked perfectly within the critical TVB-N range of the chicken. Therefore, BNC-2PVA/GSE@ZIF-8 films were selected for monitoring food freshness in this research study.

Table 3. 4 Color response to ammonia results of two-layered film

Ammonia concentration (mg/100 g)	Film images	*L**	*a**	*b**	ΔE
0		48.40±3.58^{ab}	22.20±4.08^{a}	-4.60±0.55^{a}	-
3		45.60±0.89^{b}	21.60±1.14^{a}	-5.40±0.55^{ad}	3.24±0.58^{a}
7		48.00±1.22^{b}	20.00±0.71^{ab}	-6.00±0.71^{ad}	2.93±0.64^{a}
15		50.80±3.11^{ab}	16.20±3.11^{b}	-5.40±0.55^{ad}	7.20±2.79^{b}
30		45.60±2.30^{b}	-5.20±1.30^{c}	-18.60±1.34^{b}	31.15±0.28^{c}
60		48.00±4.63^{b}	-18.00±0.71^{d}	-11.60±1.14^{c}	41.03±0.59^{d}
120		53.80±1.78^{a}	-19.20±0.45^{d}	-7.20±1.30^{d}	41.95±0.39^{d}

color and *L*, a*, b** values of three layered BNC-3PVA/GSE@ZIF-8 films are given in Table 3.5. There was no significant change of colors; ΔE values were observed in BNC-3PVA/GSE@ZIF-8 films before the ammonia concentration of 60 mg N/100 g. These films had the poorest color response and sensitivity of all the tested films. A study evaluated that the number of layers affects the response and recovery durations of pH sensors used for gas detection. The results of the study showed that the response time of the sensing layer considerably increases with the increasing number of layers (O'Toole et al., 2009). Consequently, by varying the number of layers and, therefore the thickness of the PVA/GSE@-ZIF-8 layers, the functional ammonia sensing range of the multilayer films might be controlled.

Table 3. 5 Color response to ammonia results of three-layered film

Ammonia concentration (mg/100 g)	Film images	*L**	*a**	*b**	ΔE
0		43.40±0.89^{a}	28.80±4.09^{a}	-4.40±0.55^{ab}	-
3		44.80±3.03^{a}	25.80±3.27^{a}	-5.80±0.84^{b}	5.06±2.19^{a}
7		40.20±1.10^{a}	30.20±2.28^{a}	-2.60±34^{a}	5.31±2.54^{a}
15		43.60±2.97^{a}	26.80±2.86^{a}	-4.20±0.44^{ab}	3.66±2.35^{a}
30		41.80±1.64^{a}	30.20±2.05^{a}	-3.00±1.41^{a}	3.46±1.41^{a}
60		45.60±3.13^{ab}	-11.40±0.55^{b}	-18.40±0.89^{c}	42.72±0.63^{b}
120		51.00±5.05^{b}	-16.40±0.89^{b}	-12.80±1.78^{d}	46.84±0.88^{c}

3.3.5. Chicken Spoilage Trials with Multilayer BNC-2PVA/GSE@ZIF-8 Films

TVC is a practical and widely used microbiological method that counts the number of viable microorganisms in the food sample. TVC assessment helps to control the state of food products from the production line through distribution. TVB-N and TVC levels were applied as chemical indicators to evaluate the freshness of the chicken samples. The results of TVC levels of chicken samples in 10 days of storage are shown in Figure 3.8.a with a* values and Figure 3.8.b with ΔE values, respectively. The TVC levels were recorded to analyze the microbiological quality of the chicken samples during storage at 4°C. As displayed in Figure 3.8a, TVC values of samples significantly increased throughout 10 days of storage. After the 5 days of storage, significant changes were observed in ΔE and *a** values. According to European Law (1441/2007) regulations and Turkish Standards (TS 24019:2014), the acceptable

level of TVC is set to 6.7 log CFU/g for poultry meat. This maximum limit was exceeded on day 6 of storage at 4^{o}C.

The amount of TVB-N, a chemical indication of chicken quality, is correlated with the activity of the enzyme amino acid decarboxylase during spoilage (Baltic et al., 2017). TVB-N compounds are released during spoilage and that causes the formation of off-flavors in meat products. Thus, the TVB-N level is an important indicator for monitoring the freshness of raw poultry, meat, and fishery products. In this study, the freshness of raw chicken samples was determined by detecting TVB-N levels. TVB-N threshold limit is set to 30 mg N / 100 g for poultry by the Turkish Standard (TS2409:2014). TVB-N levels of raw chicken samples are displayed in Figure 3.8. Figure 3.8.c shows TVB-N levels with a* values and Figure 3.8.d. shows with ΔE. As mentioned previously and based on the results of color changes, BNC-2PVA/GSE@ZIF-8 film was selected for monitoring food freshness.

In investigating the colorimetric responses, the color of BNC-2PVA/GSE@ZIF-8 films stayed reddish purple in the first 5 days of storage (Table 3.6.). A significant difference in film colors was observed on the 6th day of storage. The dark blue color was monitored after day 6. This substantial color change resulted in a significant increase in the value of ΔE. Accordingly, TVB-N level of chicken on day 6 was 32.9 mg/ 100 g and the TVC value was measured as 7.1 CFU/g, indicating the onset of spoilage for raw skinless chicken breast samples. Overall, BNC-2PVA/GSE@ZIF-8 film color, and consequently, its a^* and ΔE values, considerably changed concurrently with the changes in TVC and TVB-N levels at the onset of the deterioration.

These observations were in line with the research of Tang and Yu (2020) on chicken meat freshness. TVB-N levels based on the gas sensor array technique were examined, and after 5 days TVB-N level exceeded the 30 mg/100 g. Similar results were obtained in another study that monitors changes in TVC and TVB-N levels of the chicken breast during storage. TVC limit was reached with 6 days of storage and in TVB-N analysis, three out of four samples exceeded the limit on the 6th day (Baltic et al., 2017).

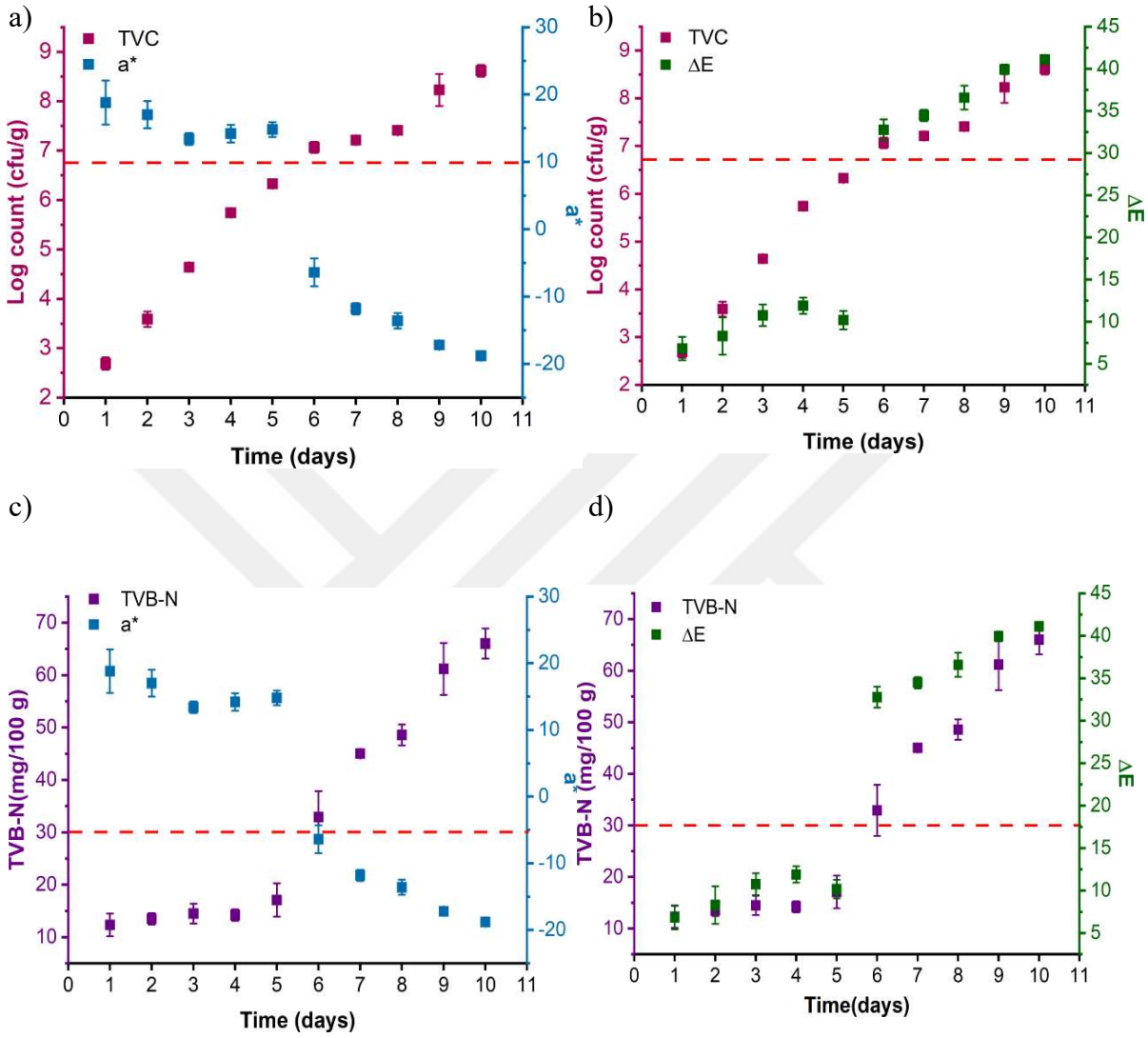

Figure 3. 8 TVC **(a)** with a* value and **(b)** with ΔE values, changes in TVB-N **(c)** with *a** value and **(d)** with ΔE values. Red dash lines show the critical limits.

Table 3. 6 The color response of BNC-2PVA/GSE@ZIF-8 film during storage at 4°C*

Storage Time (Day)	Color Response
1	
2	
3	
4	
5	
6	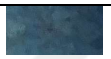
7	
8	
9	
10	

CHAPTER 4

CONCLUSIONS AND RECOMMENDATIONS

Colorimetric multilayer films composed of bacterial nanocellulose, polyvinyl alcohol, and anthocyanins-loaded ZIF-8 particles were fabricated in this study. The objective was to monitor the freshness of foods by using TVB-N sensitive color indicators. Anthocyanins were encapsulated into ZIF-8 molecules, which are highly stable and porous components since the stability of anthocyanins is considerably low while processing. The optical properties of anthocyanins and encapsulated anthocyanins were investigated to be similar. The spin coating method was used to develop PVA/GSE@ZIF-8 layers on top of the BNC layer. Characterizations of ZIF-8 and GSE@ZIF-8 show that anthocyanins were successfully encapsulated. Three different multilayer films with one layer, two layers, and three layers were tested in sensitivity, barrier, thermal, and structural characterization studies. They were examined in terms of color response to ammonia, and the film with two layers (BNC-2PVA/GSE@ZIF-8) demonstrated the best responses at the critical levels. Then, the color response of BNC-2PVA/GSE@ZIF-8 was obtained daily in parallel with TVB-N and TVC results. These findings indicate that multilayer BNC-2PVA/GSE@ZIF-8 film can differentiate fresh chicken meat from spoiled one during storage at 4 °C. The suggested technology has tremendous potential to deliver real-time data on food freshness, which could assist consumers in determining meat quality without causing damage to the food package.

For future works, anthocyanins may be obtained from a different source such as red cabbage to have better results in multilayer film colors. As red cabbage anthocyanins gives more distinctive and broad color, their spectra may be more suitable for these kind of studies.

REFERENCES

Abdullah, Z. W., & Dong, Y. (2019). Biodegradable and water resistant poly(vinyl) alcohol (pva)/starch (st)/glycerol (gl)/halloysite nanotube (HNT) nanocomposite films for Sustainable Food Packaging. *Frontiers in Materials*, *6*. https://doi.org/10.3389/fmats.2019.00058

Alizadeh-Sani, M., Mohammadian, E., Rhim, J.-W., & Jafari, S. M. (2020). Ph-sensitive (halochromic) smart packaging films based on natural food colorants for the monitoring of food quality and safety. *Trends in Food Science & Technology*, *105*, 93–144. https://doi.org/10.1016/j.tifs.2020.08.014

Andriani, D., Apriyana, A. Y., & Karina, M. (2020). The optimization of bacterial cellulose production and its applications: A Review. *Cellulose*, *27*(12), 6747–6766. https://doi.org/10.1007/s10570-020-03273-9

Annu, Ali, A., & Ahmed, S. (2021). Eco-friendly natural extract loaded Antioxidative Chitosan/polyvinyl alcohol based Active Films for Food Packaging. *Heliyon*, *7*(3). https://doi.org/10.1016/j.heliyon.2021.e06550

Ateş, S., Durmaz, E., & Hamad, A. (2016). Evaluation possibilities of cellulose derivatives in food products. *Kastamonu Üniversitesi Orman Fakültesi Dergisi*, *16*(2). https://doi.org/10.17475/kastorman.289749

Azeredo, H. M., Barud, H., Farinas, C. S., Vasconcellos, V. M., & Claro, A. M. (2019). Bacterial cellulose as a raw material for food and Food Packaging Applications. *Frontiers in Sustainable Food Systems*, *3*. https://doi.org/10.3389/fsufs.2019.00007

Balbinot-Alfaro, E., Craveiro, D. V., Lima, K. O., Costa, H. L., Lopes, D. R., & Prentice, C. (2019). Intelligent packaging with ph indicator potential. *Food Engineering Reviews*, *11*(4), 235–244. https://doi.org/10.1007/s12393-019-09198-9

Banerjee, R., Furukawa, H., Britt, D., Knobler, C., O'Keeffe, M., & Yaghi, O. M. (2009). Control of pore size and functionality in isoreticular zeolitic imidazolate frameworks and their carbon dioxide selective capture properties. *Journal of the American Chemical Society*, *131*(11), 3875–3877. https://doi.org/10.1021/ja809459e

Becerril, R., Nerín, C., & Silva, F. (2021). Bring some colour to your package: Freshness indicators based on anthocyanin extracts. *Trends in Food Science & Technology*, *111*, 495–505. https://doi.org/10.1016/j.tifs.2021.02.042

Bhagabati, P., Bhardwaj, U., & Katiyar, V. (2020). 2. Biobased and biodegradable polymers for food packaging: Commercial status. *Sustainable Polymers for Food Packaging*, 15–22. https://doi.org/10.1515/9783110648034-002

Boonsiriwit, A., Lee, M., Kim, M., Inthamat, P., Siripatrawan, U., & Lee, Y. S. (2021). Hydroxypropyl methylcellulose/microcrystalline cellulose biocomposite film incorporated with butterfly pea anthocyanin as a sustainable PH-responsive indicator for intelligent food-packaging applications. *Food Bioscience*, *44*, 101392. https://doi.org/10.1016/j.fbio.2021.101392

Borkar, R., Waghmare, S. S., & Arfin, T. (2017). Bacterial cellulose and polyester hydrogel matrices in biotechnology and biomedicine: Current status and future prospects. *Nanocellulose and Nanohydrogel Matrices*, 21–46. https://doi.org/10.1002/9783527803835.ch2

Brough, C., Miller, D. A., Ellenberger, D., Lubda, D., & Williams, R. O. (2016). Use of polyvinyl alcohol as a solubility enhancing polymer for poorly water-soluble drug delivery (part 2). *AAPS PharmSciTech*, *17*(1), 180–190. https://doi.org/10.1208/s12249-016-0490-6

Buruaga-Ramiro, C., Valenzuela, S. V., Valls, C., Roncero, M. B., Pastor, F. I. J., Díaz, P., & Martinez, J. (2020). Development of an antimicrobial bioactive paper made from bacterial cellulose. *International Journal of Biological Macromolecules*, *158*, 587–594. https://doi.org/10.1016/j.ijbiomac.2020.04.234

Cabañas-Romero, L. V., Valls, C., Valenzuela, S. V., Roncero, M. B., Pastor, F. I., Diaz, P., & Martínez, J. (2020). Bacterial cellulose–chitosan paper with antimicrobial and antioxidant activities. *Biomacromolecules*, *21*(4), 1568–1577. https://doi.org/10.1021/acs.biomac.0c00127

Calva-Estrada, S. J., Jiménez-Fernández, M., & Lugo-Cervantes, E. (2022). Betalains and their applications in food: The current state of processing, stability and future opportunities in the industry. *Food Chemistry: Molecular Sciences*, *4*, 100089. https://doi.org/10.1016/j.fochms.2022.100089

Castañeda-Ovando, A., Pacheco-Hernández, M. de, Páez-Hernández, M. E., Rodríguez, J. A., & Galán-Vidal, C. A. (2009). Chemical Studies of anthocyanins: A Review. *Food Chemistry*, *113*(4), 859–871. https://doi.org/10.1016/j.foodchem.2008.09.001

Cazón, P., & Vázquez, M. (2021). Bacterial cellulose as a biodegradable food packaging material: A Review. *Food Hydrocolloids*, *113*, 106530. https://doi.org/10.1016/j.foodhyd.2020.106530

Chandrasekhar, J., Madhusudhan, M., & Raghavarao, K. (2012). Extraction of anthocyanins from red cabbage and purification using adsorption. *Food and Bioproducts Processing, 90*(4), 615-623. doi:10.1016/j.fbp.2012.07.004

Chayavanich, K., Thiraphibundet, P., & Imyim, A. (2020). Biocompatible film sensors containing red radish extract for meat spoilage observation. *Spectrochimica Acta Part A: Molecular and Biomolecular Spectroscopy, 226*, 117601. doi:10.1016/j.saa.2019.117601

Chen, J. L., & Yan, X. P. (2011). Ionic strength and pH reversible response of visible and near-infrared fluorescence of graphene oxide nanosheets for monitoring the extracellular pH. Chemical Communications, 47(11), 3135–3137. https://doi.org/10.1039/c0cc03999c

Cheng, W., Tang, X., Zhang, Y., Wu, D., & Yang, W. (2021). Applications of metal-organic framework (MOF)-based sensors for Food Safety: Enhancing mechanisms and recent advances. *Trends in Food Science & Technology*, *112*, 268–282. https://doi.org/10.1016/j.tifs.2021.04.004

Cheng, J., Wang, H., Xiao, F., Xia, L., Li, L., & Jiang, S. (2021). Functional effectiveness of double essential oils@yam starch/microcrystalline cellulose as active antibacterial packaging. *International Journal of Biological Macromolecules*, *186*, 873–885. https://doi.org/10.1016/j.ijbiomac.2021.07.094

Chirra, S., Wang, L.-F., Aggarwal, H., Tsai, M.-F., Soorian, S. S., Siliveri, S., Goskula, S., Gujjula, S. R., & Narayanan, V. (2021). Rapid synthesis of a novel nano-crystalline mesoporous faujasite type metal-organic framework, ZIF-8 catalyst, its detailed characterization, and NABH4 assisted, enhanced catalytic rhodamine B degradation. *Materials Today Communications*, *26*, 101993. https://doi.org/10.1016/j.mtcomm.2020.101993

Choi, I., Lee, J. Y., Lacroix, M., & Han, J. (2017). Intelligent ph indicator film composed of agar/potato starch and anthocyanin extracts from purple sweet potato. *Food Chemistry, 218*, 122-128. doi:10.1016/j.foodchem.2016.09.050

Chopra, S., Dhumal, S., Abeli, P., Beaudry, R., & Almenar, E. (2017). Metal-organic frameworks have utility in adsorption and release of ethylene and 1-methylcyclopropene in fresh produce packaging. *Postharvest Biology and Technology*, *130*, 48–55. https://doi.org/10.1016/j.postharvbio.2017.04.001

Cortez, R., Luna-Vital, D. A., Margulis, D., & Gonzalez de Mejia, E. (2017). Natural Pigments: Stabilization Methods of Anthocyanins for Food Applications. Comprehensive Reviews in Food Science and Food Safety, 16(1), 180–198. https://doi.org/10.1111/1541-4337.12244

Cravillon, J., Münzer, S., Lohmeier, S.-J., Feldhoff, A., Huber, K., & Wiebcke, M. (2009). Rapid room-temperature synthesis and characterization of nanocrystals of a prototypical zeolitic imidazolate framework. *Chemistry of Materials*, *21*(8), 1410–1412. https://doi.org/10.1021/cm900166h

Dainelli, D., Gontard, N., Spyropoulos, D., Zondervan-van den Beuken, E., & Tobback, P. (2008). Active and intelligent food packaging: legal aspects and safety concerns. Trends in Food Science and Technology, 19(SUPPL. 1), S103–S112. https://doi.org/10.1016/j.tifs.2008.09.011

Dash, K. K., Deka, P., Bangar, S. P., Chaudhary, V., Trif, M., & Rusu, A. (2022). Applications of Inorganic Nanoparticles in Food Packaging: A Comprehensive Review. Polymers, 14(3), 1–20. https://doi.org/10.3390/polym14030521

Delgado-Vargas, F., Jiménez, A. R., Paredes-López, O., & Francis, F. J. (2000). 56 Natural pigments: Carotenoids, anthocyanins, and betalains - Characteristics, biosynthesis, processing, and stability. In Critical Reviews in Food Science and Nutrition (Vol. 40, Issue 3). https://doi.org/10.1080/10408690091189257

Di Filippo, M. F., Dolci, L. S., Liccardo, L., Bigi, A., Bonvicini, F., Gentilomi, G. A., Passerini, N., Panzavolta, S., & Albertini, B. (2021). Cellulose derivatives-snail slime films: New disposable eco-friendly materials for food packaging. *Food Hydrocolloids*, *111*, 106247. https://doi.org/10.1016/j.foodhyd.2020.106247

Dima, S.-O., Panaitescu, D.-M., Orban, C., Ghiurea, M., Doncea, S.-M., Fierascu, R., Nistor, C., Alexandrescu, E., Nicolae, C.-A., Trică, B., Moraru, A., & Oancea, F. (2017). Bacterial nanocellulose from side-streams of kombucha beverages production: Preparation and physical-chemical properties. *Polymers*, *9*(12), 374. https://doi.org/10.3390/polym9080374

Ding, L., Li, X., Hu, L., Zhang, Y., Jiang, Y., Mao, Z., Xu, H., Wang, B., Feng, X., & Sui, X. (2020). A naked-eye detection polyvinyl alcohol/cellulose-based ph sensor for intelligent packaging. *Carbohydrate Polymers*, *233*, 115859. https://doi.org/10.1016/j.carbpol.2020.115859

Dirpan, A., Latief, R., Syarifuddin, A., Rahman, A. N., Putra, R. P., & Hidayat, S. H. (2018). The use of colour indicator as a smart packaging system for evaluating Mangoes Arummanis (*mangifera indica* L. var. Arummanisa) freshness. *IOP Conference Series: Earth and Environmental Science*, *157*, 012031. https://doi.org/10.1088/1755-1315/157/1/012031

Drago, E., Campardelli, R., Pettinato, M., & Perego, P. (2020). Innovations in smart packaging concepts for food: An extensive review. Foods, 9(11). https://doi.org/10.3390/foods9111628

Dutra Resem Brizio, A. P. (2016). Use of Indicators in Intelligent Food Packaging. In Reference Module in Food Science (pp. 1–5). Elsevier. https://doi.org/10.1016/B978-0-08-100596-5.03214-5

Ebrahimi Tirtashi, F., Moradi, M., Tajik, H., Forough, M., Ezati, P., & Kuswandi, B. (2019). Cellulose/chitosan ph-responsive indicator incorporated with carrot anthocyanins for intelligent food packaging. *International Journal of Biological Macromolecules, 136*, 920-926. doi:10.1016/j.ijbiomac.2019.06.148

Focker, M., van Asselt, E. D., Berendsen, B. J. A., van de Schans, M. G. M., van Leeuwen, S. P. J., Visser, S. M., & van der Fels-Klerx, H. J. (2022). Review of food safety hazards in circular food systems in Europe. *Food Research International*, *158*, 111505. https://doi.org/10.1016/j.foodres.2022.111505

Fuertes, G., Soto, I., Carrasco, R., Vargas, M., Sabattin, J., & Lagos, C. (2016). Intelligent packaging systems: Sensors AND Nanosensors to Monitor food quality and safety. *Journal of Sensors, 2016*, 1-8. doi:10.1155/2016/4046061

Fung, F., Wang, H.-S., & Menon, S. (2018). Food safety in the 21st Century. *Biomedical Journal*, *41*(2), 88–95. https://doi.org/10.1016/j.bj.2018.03.003

García Ibarra, V., Sendón, R., & Rodríguez-Bernaldo de Quirós, A. (2016). Antimicrobial food packaging based on biodegradable materials. *Antimicrobial Food Packaging*, 363–384. https://doi.org/10.1016/b978-0-12-800723-5.00029-2

González, R. M., & Villanueva, M. P. (2011). Starch-based polymers for food packaging. *Multifunctional and Nanoreinforced Polymers for Food Packaging*, 527–570. https://doi.org/10.1533/9780857092786.4.527

Han, J.-W., Ruiz-Garcia, L., Qian, J.-P., & Yang, X.-T. (2018). Food packaging: A comprehensive review and future trends. *Comprehensive Reviews in Food Science and Food Safety*, *17*(4), 860–877. https://doi.org/10.1111/1541-4337.12343

He, X., Lu, W., Sun, C., Khalesi, H., Mata, A., Andaleeb, R., & Fang, Y. (2021). Cellulose and cellulose derivatives: Different colloidal states and food-related applications. *Carbohydrate Polymers*, *255*, 117334. https://doi.org/10.1016/j.carbpol.2020.117334

Heise, K., Kontturi, E., Allahverdiyeva, Y., Tammelin, T., Linder, M. B., Nonappa, & Ikkala, O. (2020). Nanocellulose: Recent fundamental advances and emerging biological and biomimicking applications. *Advanced Materials*, *33*(3), 2004349. https://doi.org/10.1002/adma.202004349

Hu, X., Yan, X., Zhou, M., & Komarneni, S. (2016). One-step synthesis of nanostructured mesoporous zif-8/silica composites. *Microporous and Mesoporous Materials*, *219*, 311–316. https://doi.org/10.1016/j.micromeso.2015.06.046

Imran, M., Klouj, A., Revol-Junelles, A.-M., & Desobry, S. (2014). Controlled release of Nisin from HPMC, sodium caseinate, poly-lactic acid and chitosan for active packaging applications. *Journal of Food Engineering*, *143*, 178–185. https://doi.org/10.1016/j.jfoodeng.2014.06.040

Jacek, P., Silva, F. A., Dourado, F., Bielecki, S., & Gama, M. (2021). Optimization and characterization of bacterial Nanocellulose produced by *komagataeibacter rhaeticus* K3. *Carbohydrate Polymer Technologies and Applications, 2*, 100022. doi:10.1016/j.carpta.2020.100022

Jiang, T., Ghosh, R., & Charcosset, C. (2021). Extraction, purification and applications of curcumin from Plant Materials-A Comprehensive Review. *Trends in Food Science & Technology*, *112*, 419–430. https://doi.org/10.1016/j.tifs.2021.04.015

Kale, R. D., & Gorade, V. G. (2018). Preparation of acylated microcrystalline cellulose using olive oil and its reinforcing effect on poly(lactic acid) films for packaging application. *Journal of Polymer Research*, *25*(3). https://doi.org/10.1007/s10965-018-1470-1

Kanatt, S. R., & Makwana, S. H. (2020). Development of active, water-resistant carboxymethyl cellulose-poly vinyl alcohol-aloe vera packaging film. *Carbohydrate Polymers*, *227*, 115303. https://doi.org/10.1016/j.carbpol.2019.115303

Kaur, H., Mohanta, G. C., Gupta, V., Kukkar, D., & Tyagi, S. (2017). Synthesis and characterization of zif-8 nanoparticles for controlled release of 6-mercaptopurine drug. *Journal of Drug Delivery Science and Technology, 41*, 106-112. doi:10.1016/j.jddst.2017.07.004

Kenion, G. B. (2019). Safety and legislative aspects of adhesives used in food packaging. *Reference Module in Food Science*. https://doi.org/10.1016/b978-0-08-100596-5.22631-0

Kim, H., Trinh, B. T., Kim, K. H., Moon, J., Kang, H., Jo, K., Akter, R., Jeong, J., Lim, E.-K., Jung, J., Choi, H.-S., Park, H. G., Kwon, O. S., Yoon, I., & Kang, T. (2021). Au@ZIF-8 SERS paper for food spoilage detection. *Biosensors and Bioelectronics*, *179*, 113063. https://doi.org/10.1016/j.bios.2021.113063

Kumar Gali, K., Bhagabati, P., & Katiyar, V. (2020). 1. Sustainable Polymers for Food Packaging: An introduction. *Sustainable Polymers for Food Packaging*, 1–14. https://doi.org/10.1515/9783110648034-001

Kuswandi, B., & Nurfawaidi, A. (2017). On-package dual sensors label based on ph indicators for real-time monitoring of beef freshness. *Food Control*, *82*, 91–100. https://doi.org/10.1016/j.foodcont.2017.06.028

Kuswandi, B., Wicaksono, Y., Jayus, Abdullah, A., Heng, L. Y., & Ahmad, M. (2011). Smart packaging: Sensors for monitoring of food quality and safety. Sensing and Instrumentation for Food Quality and Safety, 5(3–4), 137–146. https://doi.org/10.1007/s11694-011-9120-x

Kuswandi, B., Jayus, Restyana, A., Abdullah, A., Heng, L. Y., & Ahmad, M. (2012). A novel colorimetric food package label for fish spoilage based on polyaniline film. Food Control, 25(1), 184–189. https://doi.org/10.1016/j.foodcont.2011.10.008

Lalpuria, M., Anantheswaran, R., & Floros, J. (2012). Packaging Technologies and their role in Food Safety. *Microbial Decontamination in the Food Industry*, 701–745. https://doi.org/10.1533/9780857095756.4.701

Liu, D., Zhang, C., Pu, Y., Chen, S., Li, H., & Zhong, Y. (2023). Novel colorimetric films based on polyvinyl alcohol/sodium carboxymethyl cellulose doped with anthocyanins and betacyanins to monitor pork freshness. *Food Chemistry*, *404*, 134426. https://doi.org/10.1016/j.foodchem.2022.134426

Liu, Y., Ahmed, S., Sameen, D. E., Wang, Y., Lu, R., Dai, J., Li, S., & Qin, W. (2021). A review of cellulose and its derivatives in biopolymer-based for Food Packaging Application. *Trends in Food Science & Technology*, *112*, 532–546. https://doi.org/10.1016/j.tifs.2021.04.016

Liu, Z., Smart, J. D., & Pannala, A. S. (2020). Recent developments in formulation design for improving oral bioavailability of curcumin: A Review. *Journal of Drug Delivery Science and Technology*, *60*, 102082. https://doi.org/10.1016/j.jddst.2020.102082

Ludwicka, K., Kaczmarek, M., & Białkowska, A. (2020). Bacterial nanocellulose—a biobased polymer for active and intelligent food packaging applications: Recent advances and developments. *Polymers*, *12*(10), 2209. https://doi.org/10.3390/polym12102209

López de Dicastillo, C., Rodríguez, F., Guarda, A., & Galotto, M. J. (2016). Antioxidant films based on cross-linked methyl cellulose and native Chilean Berry for Food Packaging Applications. *Carbohydrate Polymers*, *136*, 1052–1060. https://doi.org/10.1016/j.carbpol.2015.10.013

Ma, P., Zhang, J., Liu, P., Wang, Q., Zhang, Y., Song, K., Li, R., & Shen, L. (2020). Computer-assisted design for stable and porous metal-organic framework (MOF) as a carrier for curcumin delivery. *LWT*, *120*, 108949. https://doi.org/10.1016/j.lwt.2019.108949

Magri, A., Petriccione, M., & Gutiérrez, T. J. (2021). Metal-organic frameworks for Food Applications: A Review. *Food Chemistry*, *354*, 129533. https://doi.org/10.1016/j.foodchem.2021.129533

Mangaraj, S., Yadav, A., Bal, L. M., Dash, S. K., & Mahanti, N. K. (2018). Application of biodegradable polymers in food packaging industry: A comprehensive review. *Journal of Packaging Technology and Research*, *3*(1), 77–96. https://doi.org/10.1007/s41783-018-0049-y

Martins, V. G., Santos, L. G., Romani, V. P., & Fernandes, S. S. (2022). Chapter 3. bio-based sensing: Role of natural dyes in food freshness indicators. *Food Chemistry, Function and Analysis*, 37–62. https://doi.org/10.1039/9781839167966-00037

Merz, B., Capello, C., Leandro, G. C., Moritz, D. E., Monteiro, A. R., & Valencia, G. A. (2020). A novel colorimetric indicator film based on Chitosan, Polyvinyl Alcohol and anthocyanins from jambolan (syzygium cumini) fruit for monitoring shrimp freshness. *International Journal of Biological Macromolecules*, *153*, 625–632. https://doi.org/10.1016/j.ijbiomac.2020.03.048

Mchugh, T. H., Avena-bustillos, F. L., & Krochta, J. M. (1993). Hydrophilic Edible Films : Modified Procedure for Water Vapor Permeability and Explanation of Thickness Effects. Journal of Food Science, 58(4), 899–903. https://doi.org/https://doi.org/10.1111/j.1365-2621.1993.tb09387.x

Mohammad, SS. (2021). Anthocyanins: Chemical properties and health benefits: A Review. *Current Nutrition & Food Science*, *17*(7). https://doi.org/10.2174/15734013mteysotqs3

Mohammadalinejhad, S., Almasi, H., & Moradi, M. (2020). Immobilization of echium amoenum anthocyanins into bacterial cellulose film: A novel colorimetric ph indicator for freshness/spoilage monitoring of shrimp. *Food Control*, *113*, 107169. https://doi.org/10.1016/j.foodcont.2020.107169

Moradi, M., Tajik, H., Almasi, H., Forough, M., & Ezati, P. (2019). A novel ph-sensing indicator based on bacterial cellulose nanofibers and black carrot anthocyanins for monitoring fish freshness. *Carbohydrate Polymers*, *222*, 115030. https://doi.org/10.1016/j.carbpol.2019.115030

Morán, J. I., Alvarez, V. A., Cyras, V. P., & Vázquez, A. (2007). Extraction of cellulose and preparation of nanocellulose from sisal fibers. *Cellulose*, *15*(1), 149–159. https://doi.org/10.1007/s10570-007-9145-9

Mu, R., Hong, X., Ni, Y., Li, Y., Pang, J., Wang, Q., Xiao, J., & Zheng, Y. (2019). Recent trends and applications of cellulose nanocrystals in food industry. *Trends in Food Science & Technology*, *93*, 136–144. https://doi.org/10.1016/j.tifs.2019.09.013

Muppalla, S. R., Kanatt, S. R., Chawla, S. P., & Sharma, A. (2014). Carboxymethyl cellulose–polyvinyl alcohol films with clove oil for active packaging of ground chicken meat. *Food Packaging and Shelf Life*, *2*(2), 51–58. https://doi.org/10.1016/j.fpsl.2014.07.002

Müller, P., & Schmid, M. (2019). Intelligent packaging in the food sector: A brief overview. Foods, 8(1). https://doi.org/10.3390/foods8010016

Nadar, S. S., & Rathod, V. K. (2020). Immobilization of proline activated lipase within Metal Organic Framework (MOF). *International Journal of Biological Macromolecules*, *152*, 1108–1112. https://doi.org/10.1016/j.ijbiomac.2019.10.199

Naduparambath, S., T.V., J., V., S., M.P., S., Balan, A. K., & E., P. (2018). Isolation and characterisation of cellulose nanocrystals from sago seed shells. *Carbohydrate Polymers*, *180*, 13–20. https://doi.org/10.1016/j.carbpol.2017.09.088

Naseer, S., Hussain, S., & Abid, A. (2019). Betalain as a food colorant: Its sources, chemistry and health benefits. Proceedings of the Pakistan Academy of Sciences: Part B, 56(2), 1–8.

Navarro, J., Almora Barrios, N., Lerma Berlanga, B., Ruiz-Pernía, J. J., Lorenz Fonfria, V. A., Tuñón, I., & Martí-Gastaldo, C. (2019). Translocation of enzymes into a mesoporous MOF for enhanced catalytic activity under extreme conditions. *Chemical Science*. https://doi.org/10.1039/c9sc00082h

Park, K. S., Ni, Z., Côté, A. P., Choi, J. Y., Huang, R., Uribe-Romo, F. J., Chae, H. K., O'Keeffe, M., & Yaghi, O. M. (2006). Exceptional Chemical and thermal stability of zeolitic imidazolate frameworks. *Proceedings of the National Academy of Sciences*, *103*(27), 10186–10191. https://doi.org/10.1073/pnas.0602439103

Pereira, V. A., de Arruda, I. N., & Stefani, R. (2015). Active chitosan/PVA films with anthocyanins from Brassica Oleraceae (red cabbage) as time–temperature indicators for application in Intelligent Food Packaging. *Food Hydrocolloids*, *43*, 180–188. https://doi.org/10.1016/j.foodhyd.2014.05.014

Prietto, L., Mirapalhete, T. C., Pinto, V. Z., Hoffmann, J. F., Vanier, N. L., Lim, L.-T., Guerra Dias, A. R., & da Rosa Zavareze, E. (2017). Ph-sensitive films containing anthocyanins extracted from black bean seed coat and red cabbage. *LWT*, *80*, 492–500. https://doi.org/10.1016/j.lwt.2017.03.006

Realini, C. E., & Marcos, B. (2014). Active and intelligent packaging systems for a modern society. Meat Science, 98(3), 404–419. https://doi.org/10.1016/j.meatsci.2014.06.031

Rodriguez-Amaya, D. B. (2019). Update on natural food pigments - a mini-review on carotenoids, anthocyanins, and betalains. *Food Research International*, *124*, 200–205. https://doi.org/10.1016/j.foodres.2018.05.028

Rhim, J. W., & Ng, P. K. W. (2007). Natural biopolymer-based nanocomposite films for packaging applications. Critical Reviews in Food Science and Nutrition, 47(4), 411–433. https://doi.org/10.1080/10408390600846366

Rukchon, C., Nopwinyuwong, A., Trevanich, S., Jinkarn, T., & Suppakul, P. (2014). Development of a food spoilage indicator for monitoring freshness of skinless chicken breast. Talanta, 130, 547–554. https://doi.org/10.1016/j.talanta.2014.07.048

Sandra Hoffmann and Jae-Wan Ahn. (2021). *Updating economic burden of foodborne diseases estimates for inflation and income growth*. USDA ERS. Retrieved from https://www.ers.usda.gov/publications/pub-details/?pubid=102639

Sarwar, M. S., Niazi, M. B., Jahan, Z., Ahmad, T., & Hussain, A. (2018). Preparation and characterization of PVA/nanocellulose/AG nanocomposite films for Antimicrobial Food Packaging. *Carbohydrate Polymers*, *184*, 453–464. https://doi.org/10.1016/j.carbpol.2017.12.068

Schaefer, D., & Cheung, W. M. (2018). Smart packaging: Opportunities and challenges. *Procedia CIRP*, *72*, 1022–1027. https://doi.org/10.1016/j.procir.2018.03.240

Shao, P., Liu, L., Yu, J., Lin, Y., Gao, H., Chen, H., & Sun, P. (2021). An overview of intelligent freshness indicator packaging for food quality and safety monitoring. *Trends in Food Science & Technology*, *118*, 285–296. https://doi.org/10.1016/j.tifs.2021.10.012

Smeriglio, A., Barreca, D., Bellocco, E., & Trombetta, D. (2016). Chemistry, Pharmacology and Health Benefits of Anthocyanins. Phytotherapy Research, 1286(April), 1265–1286. https://doi.org/10.1002/ptr.5642

Sharanyakanth, P. S., & Radhakrishnan, M. (2020). Synthesis of metal-organic frameworks (mofs) and its application in Food Packaging: A critical review. *Trends in Food Science & Technology*, *104*, 102–116. https://doi.org/10.1016/j.tifs.2020.08.004

Sneddon, S., Kahr, J., Orsi, A. F., Price, D. J., Dawson, D. M., Wright, P. A., & Ashbrook, S. E. (2017). Investigation of zeolitic imidazolate frameworks using 13 C and 15 N Solid-state NMR spectroscopy. *Solid State Nuclear Magnetic Resonance, 87*, 54-64. doi:10.1016/j.ssnmr.2017.09.001

Smolander, M. (2008). Freshness indicators for food packaging. *Smart Packaging Technologies for Fast Moving Consumer Goods*, 111–127. https://doi.org/10.1002/9780470753699.ch7

Soundararajan, N., & Katiyar, V. (2020). 9. Biobased biodegradable polymers in food packaging: Regulations and legislations. *Sustainable Polymers for Food Packaging*, 159–170. https://doi.org/10.1515/9783110648034-009

Sundramoorthy, A. K., Vignesh Kumar, T. H., & Gunasekaran, S. (2018). Graphene-based nanosensors and smart food packaging systems for Food Safety and Quality Monitoring. *Graphene Bioelectronics*, 267–306. https://doi.org/10.1016/b978-0-12-813349-1.00012-3

Tajeddin, B., & Arabkhedri, M. (2020). Polymers and food packaging. *Polymer Science and Innovative Applications*, 525–543. https://doi.org/10.1016/b978-0-12-816808-0.00016-0

Tang, X., & Yu, Z. (2020). Rapid evaluation of chicken meat freshness using gas sensor array and signal analysis considering total volatile basic nitrogen. *International Journal of Food Properties*, *23*(1), 297–305. https://doi.org/10.1080/10942912.2020.1716797

Tian, F., Cerro, A. M., Mosier, A. M., Wayment-Steele, H. K., Shine, R. S., Park, A., . . . Benz, L. (2014). Surface and stability characterization of a nanoporous zif-8 thin film. *The Journal of Physical Chemistry C, 118*(26), 14449-14456. doi:10.1021/jp5041053

Tiwari, A., Singh, A., Garg, N., & Randhawa, J. K. (2017). Curcumin encapsulated zeolitic imidazolate frameworks as stimuli responsive drug delivery system and their interaction with biomimetic environment. *Scientific Reports*, *7*(1). https://doi.org/10.1038/s41598-017-12786-6

Trache, D., Hussin, M. H., Hui Chuin, C. T., Sabar, S., Fazita, M. R. N., Taiwo, O. F. A., Hassan, T. M., & Haafiz, M. K. M. (2016). Microcrystalline cellulose: Isolation, characterization and bio-composites application—a review. *International Journal of Biological Macromolecules*, *93*, 789–804. https://doi.org/10.1016/j.ijbiomac.2016.09.056

Vanderroost, M., Ragaert, P., Devlieghere, F., & De Meulenaer, B. (2014). Intelligent Food Packaging: The next generation. *Trends in Food Science & Technology*, *39*(1), 47–62. https://doi.org/10.1016/j.tifs.2014.06.009

Vinha, A. F., Rodrigues, F., Nunes, M. A., & Oliveira, M. B. P. P. (2018). Natural pigments and colorants in foods and beverages. In Polyphenols: Properties, Recovery, and Applications. Elsevier Inc. https://doi.org/10.1016/B978-0-12-813572-3.00011-7

Wallace, T. C., & Giusti, M. M. (2019). Anthocyanins—nature's bold, beautiful, and health-promoting colors. *Foods*, *8*(11), 550. https://doi.org/10.3390/foods8110550

Wang, H., Lashkari, E., Lim, H., Zheng, C., Emge, T. J., Gong, Q., Yam, K., & Li, J. (2016). The moisture-triggered controlled release of a natural food preservative from a microporous metal–organic framework. *Chemical Communications*, *52*(10), 2129–2132. https://doi.org/10.1039/c5cc09634k

Wang, P.-L., Xie, L.-H., Joseph, E. A., Li, J.-R., Su, X.-O., & Zhou, H.-C. (2019). Metal–organic frameworks for Food Safety. *Chemical Reviews*, *119*(18), 10638–10690. https://doi.org/10.1021/acs.chemrev.9b00257

Wu, Y., Luo, Y., Zhou, B., Mei, L., Wang, Q., & Zhang, B. (2019). Porous metal-organic framework (MOF) carrier for incorporation of volatile antimicrobial essential oil. *Food Control*, *98*, 174–178. https://doi.org/10.1016/j.foodcont.2018.11.011

Wu, Y., Ying, Y., Liu, Y., Zhang, H., & Huang, J. (2018). Preparation of chitosan/poly vinyl alcohol films and their inhibition of biofilm formation against pseudomonas aeruginosa pao1. *International Journal of Biological Macromolecules, 118*, 2131-2137. doi:10.1016/j.ijbiomac.2018.07.061

Yam, K. L. (2012). Intelligent packaging to enhance food safety and quality. *Emerging Food Packaging Technologies*, 137–152. https://doi.org/10.1533/9780857095664.2.137

Yildiz, E., Sumnu, G., & Kahyaoglu, L. N. (2021). Monitoring freshness of chicken breast by using natural halochromic curcumin loaded chitosan/PEO nanofibers as an intelligent package. International Journal of Biological Macromolecules, 170, 437–446.

Young, E., Mirosa, M., & Bremer, P. (2020). A systematic review of consumer perceptions of smart packaging technologies for food. Frontiers in Sustainable Food Systems, 4(May), 1–20. https://doi.org/10.3389/fsufs.2020.00063

Yousefi, H., Su, H.-M., Imani, S. M., Alkhaldi, K., M. Filipe, C. D., & Didar, T. F. (2019). Intelligent Food Packaging: A review of smart sensing technologies for Monitoring Food Quality. *ACS Sensors*, *4*(4), 808–821. https://doi.org/10.1021/acssensors.9b00440

Zhai, X., Shi, J., Zou, X., Wang, S., Jiang, C., Zhang, J., Huang, X., Zhang, W., & Holmes, M. (2017). Novel colorimetric films based on starch/polyvinyl alcohol incorporated with roselle anthocyanins for fish freshness monitoring. Food Hydrocolloids, 69, 308–317. https://doi.org/10.1016/j.foodhyd.2017.02.014

Zhao, C.-L., Yu, Y.-Q., Chen, Z.-J., Wen, G.-S., Wei, F.-G., Zheng, Q., Wang, C.-D., & Xiao, X.-L. (2017). Stability-increasing effects of anthocyanin glycosyl acylation. *Food Chemistry*, *214*, 119–128. https://doi.org/10.1016/j.foodchem.2016.07.073

Zhao, J., Wei, F., Xu, W., & Han, X. (2020). Enhanced antibacterial performance of gelatin/chitosan film containing capsaicin loaded mofs for food packaging. *Applied Surface Science*, *510*, 145418. https://doi.org/10.1016/j.apsusc.2020.145418

Zheng, G., Chen, Z., Sentosun, K., Pérez-Juste, I., Bals, S., Liz-Marzán, L. M., Pastoriza-Santos, I., Pérez-Juste, J., & Hong, M. (2017). Shape control in zif-8 nanocrystals and metal nanoparticles@ZIF-8 heterostructures. *Nanoscale*, *9*(43), 16645–16651. https://doi.org/10.1039/c7nr03739b

Zhou, H.-C., Long, J. R., & Yaghi, O. M. (2012). Introduction to metal–organic frameworks. *Chemical Reviews*, *112*(2), 673–674. https://doi.org/10.1021/cr300014x

APPENDICES

A. Statistical Analysis

Table 1. WS of multilayer films

	N	Mean	Standart Deviation
BNC	3	0.0793	0.0389
BNC-1PVA/GSE@ZIF-8	3	0.1845	0.0571
BNC-2PVA/GSE@ZIF-8	3	0.2853	0.045
BNC-3PVA/GSE@ZIF-8	3	0.3094	0.0461

Tukey Test

	Mean	Grouping		
BNC	0.0793	A		
BNC-1PVA/GSE@ZIF-8	0.1845	A	B	
BNC-2PVA/GSE@ZIF-8	0.2853		B	C
BNC-3PVA/GSE@ZIF-8	0.3094			C

Table 2. Thickness of multilayer films

	N	Mean	Standart Deviation
BNC	3	0.013	0.001
BNC-1PVA/GSE@ZIF-8	3	0.017	0.003
BNC-2PVA/GSE@ZIF-8	3	0.026	0.003
BNC-3PVA/GSE@ZIF-8	3	0.031	0.002

Tukey Test

	Mean	Grouping
BNC	0.013	A
BNC-1PVA/GSE@ZIF-8	0.017	A
BNC-2PVA/GSE@ZIF-8	0.026	B
BNC-3PVA/GSE@ZIF-8	0.031	B

Table 3. WVP of multilayer films

	N	Mean	Standart Deviation
BNC	3	5.33	0.27
BNC-1PVA/GSE@ZIF-8	3	6.81	0.8
BNC-2PVA/GSE@ZIF-8	3	9.96	0.55
BNC-3PVA/GSE@ZIF-8	3	10.8	0.38

Tukey Test

	Mean	Grouping
BNC	5.33	A
BNC-1PVA/GSE@ZIF-8	6.81	B
BNC-2PVA/GSE@ZIF-8	9.96	C
BNC-3PVA/GSE@ZIF-8	10.8	C

Table 4. ΔE values of BNC-1PVA/GSE@ZIF-8 films in response of ammonia

Ammonia concentration (mg/100 g)	N	Mean	Standart Deviation
0	3	0	0.00
3	3	3.95	0.66
7	3	17.33	0.69
15	3	23.66	1.88
30	3	26.37	1.90
60	3	28.16	2.05
120	3	27.19	2.43

Tukey Test

Ammonia concentration (mg/100 g)	Mean	Grouping		
0	0	-		
3	3.95	A		
7	17.33		B	
15	23.66			C
30	26.37			C D
60	28.16			D
120	27.19			C D

Table 5. ΔE values of BNC-2PVA/GSE@ZIF-8 films in response of ammonia

Ammonia concentration (mg/100 g)	N	Mean	Standart Deviation
0	3	0	0.00
3	3	3.24	0.58
7	3	2.93	0.64
15	3	7.2	2.79
30	3	31.15	0.28
60	3	41.03	0.59
120	3	41.95	0.39

Tukey Test

Ammonia concentration (mg/100 g)	Mean	Grouping
0	0	-
3	3.24	A
7	2.93	A
15	7.2	B
30	31.15	C
60	41.03	D
120	41.95	D

Table 6. ΔE values of BNC-3PVA/GSE@ZIF-8 films in response of ammonia

Ammonia concentration (mg/100 g)	N	Mean	Standart Deviation
0	3	0	0.00
3	3	5.06	2.19
7	3	5.31	2.54
15	3	3.66	2.35
30	3	3.46	1.41
60	3	42.72	0.63
120	3	46.84	0.88

Tukey Test

Ammonia concentration (mg/100 g)	Mean	Grouping
0	0	-
3	5.06	A
7	5.31	A
15	3.66	A
30	3.46	A
60	42.72	B
120	46.84	B

Table 4. TVB-N of chicken samples

	N	Mean	Standart Deviation
Day 1	2	11.24	1.31
Day 2	2	13.02	0.26
Day 3	2	14.72	1.18
Day 4	2	14.54	0.31
Day 5	2	17.79	2.23
Day 6	2	32.38	3.35
Day 7	2	44.95	0.11
Day 8	2	48.52	1.22
Day 9	2	61.21	3.48
Day 10	2	65.98	1.97

Tukey Test

	Mean	Grouping
Day 10	65.98	A
Day 9	61.21	B
Day 8	48.52	C
Day 7	44.95	D
Day 6	32.38	E
Day 5	17.79	F
Day 4	14.54	G
Day 3	14.72	H
Day 2	13.02	I
Day 1	11.24	J